Air-Water Interface Flows in Pipe Emptying

by

Malusi Fana Dlamini

A thesis submitted to the Graduate Faculty of
Auburn University
in partial fulfillment of the
requirements for the Degree of
Master of Science

Auburn, Alabama
August 08, 2020

Water pipelines, Air ventilation, Experimental investigation, Numerical Modeling

Approved by

Jose Goes Vasconcelos, Chair, Associate Professor of Civil Engineering
Xing Fang, Professor of Civil Engineering
Frances O'Donnell, Assistant Professor of Civil Engineering

Abstract

Pipe emptying is an important component of water supply operations. Pipes can be drained as a scheduled operation preceding maintenance, flushed for health reasons or they may empty as a result of an accidental break causing flooding to the surroundings. The critical parameters to consider when a pipe is drained are the sub-atmospheric pressure variations and flow rate. Sub-atmospheric pressure can cause damage on the pipeline installations as well as the pipeline itself, while flow rates can cause flooding if not adequately controlled. This paper presents laboratory experiments that were carried out to observe the air-water interfaces as well as record the pressure changes and outflow rates. These were generated by systematic variations in slope, ventilation and discharge port. The results are compared with those of Zukoski (1966), Benjamin (1968), Baines (1991) and the orifice equation. The interfaces can generally be divided into five major groups, gulping, near horizontal, gravity current, dual gravity current and combination of gravity current and near horizontal. The initiation of discharge resulted in sub-atmospheric pressure upstream. The combination of no ventilation, maximum discharge port and steepest slope produced the largest sub-atmospheric pressure. Maximum flow rate was produced from steepest slope, maximum discharge port and largest ventilation. A Runge-Kutta 4^{th} order model utilizing the rigid column theory is also presented to assess the ability of such simplifying modeling approaches to explain the pressure variations and flow rates.

Acknowledgments

I would like to thank my advisor, Professor Jose Vasconcelos, for guiding me and offering professional and personal advice from the first time I came to Auburn, Alabama. I would also like to thank him for displaying extreme patience and knowledge as we worked tirelessly to produce this research. His great insight into interface flows and numerical modeling was valuable. It helped me navigate fields I had not encountered before but now I can dare to tackle on my own. I would also like to thank Jalil Jamily for all the assistance in the laboratory with the experiments and even the little things that make the whole experience better.

I would also like to thank my family, Nomahlubi (wife), Yanis and Yanai my sons, for all the encouragement and sacrifice they had to endure for me to be here. The sad moments, laughter, joyful moments all made this an experience I will treasure for a lifetime. Your support was invaluable, thank you from the bottom of my heart.

Thank you to all my Auburn family, special thanks to Susi and Mark Grantham, Matt and April Dean, Jack and Kelly Somers and Kerry and Laura Bradley, you made my stay here worthwhile. I cannot even imagine how I would have gone through the two years without you. Special mention my colleagues to Bushra Tasnim and Meredith Ayers, you were amazing.

Finally thank to Fulbright for affording me the opportunity to study in the United States, it has been an honor

Table of Contents

List of Figures

List of Tables

List of Abbreviations

A	Water flow cross-sectional area
Ae	Area of Ellipse
A_o	Normalized discharge orifice
A_v	Normalized ventilation orifice
c	celerity
C	Flooding coefficient
C_d	Orifice discharge coefficient (assumed 0.65)
d	ventilation diameter
D	Internal pipe diameter
f	friction head loss
g	acceleration due to gravity
H	Height of duct
h_s	Length of vertical pipe
H_{air}	Air pressure,
H_{abs}	Absolute air pressure head

h_p Pressure head difference

H_{atm} Atmospheric pressure head.

K Polytropic exponent

L_{tail} Tailing water behind the air front head

L_e Length of emptying water column

L_w Length of water column

P_A Pressure at point A

W Weight of water

V_f Front velocity

θ Pipe inclination angle with the horizontal

y_f Gravity current depth

ρ_w Water density

ρ_a Air density

u_d velocity of cavity

v Water velocity

x Distance from origin to interface position

m_a	Air mass
β	Correction factor for momentum changes
τ_{bx}	wall shear stress
$-\overline{u'^2}$	Turbulence intensity
P_D	Pressure on top of the pipe
Q_{air}	Air flow rate
Y	Expansion factor.

Chapter 1

Introduction

Water emptying in pipeline operations is invertible. This applies to both industrial and small scale operations. Pipeline emptying is usually a complex process that requires careful planning and execution. In the planning phase of water emptying stage, knowledge of where the water will discharge to, volume of water to be drained, what pressures can be expected in the water system, how long will it take to empty the pipeline are some of the parameters that must be known. Pipeline emptying applies to different industries, food, supply, water collection, gas, oil etc, either pressurized or not pressurized. In this research focus is made to pipe emptying flows, generated by gravity for water supply systems.

Two phase pipe flow conditions, while not desirable, occur in pipe emptying and filling operations when there is flow between fluids of different densities, in this case water and air. The two phase flows in pipe emptying has not been studied in great detail, yet this is an everyday function in different industries and services, particularly waterworks authorities. A pipeline in operation will at some point need to be emptied for scheduled or unscheduled maintenance or it may drain by accident such as failures or external damage. It is important to know the conditions that will follow these kind of operations, particularly in terms of flow regimes inside the conduits, outflow rates and internal pressures.

Intermittent water supply conditions expose water supply networks to repeated emptying and filling processes. These can be very damaging to the pipelines (Kumpel, 2016) and therefore it is important to ensure safe operation to save repair and replacement costs. One of the methods which can be used for water pipeline operations efficiency is the introduction of ventilation (air valves). In pipe emptying and filing operations, ventilation mitigates the buildup of damaging pressures inside the pipe. These pressures are negative for pipe emptying and positive for pipe filing.

Two phase flows are not desirable in pipe emptying operations. This is because of their hard to their predict behavior. It is for this reason that it is useful to know what conditions will result in this kind of flow so that they can be mitigated. This research identifies the conditions necessary for each interface flow type. This can be useful in changing the pipe flow conditions to eliminate the occurrence of the two phase flows.

This research is intended to be used in decision making by water practitioners, in the design and operating of water systems. It is also meant to assist model developers to better understand two phase flows and thus develop more accurate models with interface shapes that are more representative of the actual interfaces based on the prevailing conditions and pipe geometry. For water practitioners the numerical model will be used to decide the location and size of ventilation required to prevent excess pressures in pipe emptying. This feature can be extended to determine the pressures that can be expected in the pipeline. Pressure management can also be conducted by changing the discharge conditions. This tool is designed to be able to handle all those conditions.

1.1 Pipe emptying and ventilation

Emptying of gravity flowing pipelines will result in negative pressure at locations in higher elevations. As water flows out of pipelines at discharge points, mass conservation dictates that the discharge volume will result in sub-atmospheric conditions inside the pipe, which will typically be partially compensated with the admission of air through ventilation points. Depending on the size of the ventilation available in the system provided by air valves, and their operational conditions, these negative pressures can be large enough to create damaging internal pressures (Fuertes-Miquel et al. 2019). These are conditions that must be anticipated in water system design and operation, and motivates the present research.

The best way to mitigate the sub-atmospheric pressures is through a well-designed and maintained ventilation system (Xue and Zheng 2011). This allows more atmospheric air to enter the system to fill the volume created by the water displacement. This has been studied in recent times by Coronado-Hernández et al. (2017) and Fuertes-Miquel et al. (2019) with the goal of finding the best size ventilation or air valves to ensure minimal disruption to flows. Further knowledge of these upstream pressures can also help in the selection of pipe material to use in the design and construction of water supply systems. This is because materials and material thickness are chosen based on expected pressures the system will be subjected to. Flow rates knowledge is usually limited before the start of pipe draining operations. To our knowledge, there has been no systematic investigation on air-water interfaces in closed conduits undergoing emptying. Without this

knowledge, one cannot ascertain the applicability of modeling tools to describe and predict such events. This point is further developed in the subsequent sections.

1.2 Air-Water interfaces in pipe emptying conditions

An important factor to consider in interface flows is the interface shape and characteristics. These are important because they determine the kind of mathematical model and related flow assumptions that can be applied. Current research has indicated three main types of air-water interfaces in closed conduits undergoing emptying:

- Gravity currents (Baines 1991; Benjamin 1968; Zukoski 1966).
- Gulping (Geiger et al. 2012; Kordestani and Kubie 1996)
- Near-horizontal interfaces (Coronado-Hernández et al. 2018; Nicholson et al. 1978).

The experimental investigation is an adequate method to gain insights on the air-water interface characteristics during emptying processes. This is because it provides both visual and experimental data and because of the possibility of having a systematic variability of testing conditions. Yet, there is a limited amount of experimental data concerning pipeline emptying processes. For sloped conduits, one of the pioneering and most useful dataset available was presented by Zukoski (1966) but even this dataset involved only relatively small diameters and slopes exceeding 10 degrees. Vertical pipes without ventilation have been studied in different contributions Batchelor (1967); McQuillan and Whalley (1985); Kordestani and Kubie (1996); Clanet and Searby (2004); Mer et al. (2018), but these have significantly different behavior during emptying. These studies indicated

that, depending on discharge conditions, one can observe the advance of a Taylor bubble, slug flow or gulping, as is further elaborated.

1.3 Numerical modeling of pipe emptying flows

Numerical models have been developed to study and predict two phase flows for both filling and emptying processes. Xue and Zheng (2011) described these processes as the inverse of each other noting that this was especially true for horizontal pipes. This shows that for mathematical modeling, principles from pipe filling models can be manipulated and used in pipe emptying models.

The has been significant contributions to the study of ventilation in pipe operations. These studies have however concentrated on pipe filling processes for example, Vasconcelos and Wright (2008); Coronado-Hernández et al. (2018) both studied the effects ventilation in pipe filling, they also developed models to try and explain these processes. Zhou et al. (2002) and Xue and Zheng (2011) studied ventilation in horizontal pipes with constant pressure head and how different size ventilation affects the pressure in these pipes. Li et al. (2018) and Fuertes-Miquel et al. (2019) have studied ventilation valves in pipe emptying and filling operations with the aim of finding the correct size valve to be used in these operations.

Gravity controlled pipe flows form a large fraction of water supply systems because of the intentional design to avoid power costs. Many of these studies assume simplified air-water

interfaces in their formulation, but it is fundamentally important to assess whether these assumptions are valid.

1.4 Motivation

At present there is no study that systematically combines geometry, ventilation degree and discharge conditions in closed conduits undergoing emptying. On the numerical modeling side, this has impacted the development of accurate models that can be used to describe emptying process in a generic format. This has led to the slow development of easy to use models that can predict upstream pressure and interface shape and position. In another hand, the representation of geometric and outflow conditions in previous investigations was limited, as was pointed earlier, and did not include some possible conditions, such as very large openings that could represent major pipelines ruptures. Various experimental studies were focused in water outflows in either vertical or horizontal geometries, while fewer covered the range of slopes up to 10 degrees that are more typical from long water pipelines. These limitations on the available experimental data representing pipeline emptying guided the development of the research objectives.

1.5 Research objectives

This research is an experimental investigation to characterize air-water interactions in closed pipelines during emptying operations. Specifically, the research aimed to perform experimental

measurements of pressure, air-water interfaces, and outflows to assess the effect of different configurations of discharge orifice size, ventilation, and slope during the emptying processes.

1.6 Structure of the thesis

This master thesis is divided into 6 chapters as outlined below:

- Chapter 1 presents the introduction and background of the research, while also highlighting the problems, aims, and structure of the thesis
- Chapter 2 provides the literature review, focusing on the different types of interface flows and available models to deal with the problem
- Chapter 3 highlights the knowledge gaps that this research addresses.
- Chapter 4 describes the experiments performed and the apparatus used. The numerical model development to represent some of the experimental conditions is also discussed in this section.
- Chapter 5 presents the results
- Chapter 6 is the conclusion which also includes limitations from this research as well as recommendations for further work in this field

Chapter 2

Literature review

The literature review presents an overview study and available information on air-water interfaces, pipe emptying, and pipe ventilation. The pipe emptying section presents both numerical and experimental research which has been done on pipe emptying. The air-water interface flows

section discusses the propagation of air-water interface in a pipeline including the different interfaces formed for example gravity currents and gulping. The section on ventilation presents models, mostly from pipe filling which has influenced the pipe emptying and rigid column model development for pipe emptying.

2.1 Air water interfaces

There is a wide range of practical applications and areas in engineering that focuses on two-phase flows. Two-phase flow patterns are influenced by several factors ranging from pipe orientation, laminar or turbulent flow regimes, intermittent or steady inflows, geometry changes, among others. In this literature review, a general overview of such flows is presented, along with elements that indicate the similarity of the governing principles. Among the different two-phase flow regimes in closed pipes, the focus is placed on gravity currents, slug flows, and gulping flows.

2.1.1 Gravity currents

Two-phase flows have been studied for decades by different researchers. Zukoski (1966) investigated vertical and inclined bubbles advancing in closed conduits with two fluids. His focus was to study the influence of viscosity and surface tension on the propagation of these bubbles. His experimental work used liquids of different characteristics, including water, mercury, and others. Three methods were used to generate the bubbles, namely placing the filled pipe over a beaker with the same fluid and then removing the beaker and allowing the fluid to drain out. The technique used for liquid to liquid test involved filling the pipe with the two liquids, with the denser liquid at the bottom, the pipe was then suddenly inclined, and the bubble motion recorded. The

third technique placed balloons filled with air at the bottom of the pipe, these were ruptured to create an air bubble. The results of the experiment showed that the celerity of bubbles increases with decreasing slope for angles less than 90 degrees with the horizontal. A decrease in angle beyond 45 degrees results in a decrease in bubble celerity, as is illustrated in Figure 2.1

This study also found that when there is flow initiated in a pipe, the denser fluid moves to the bottom of the pipe and makes an angle proportional to the angle of inclination. Another important finding was that the pipe material does not affect the flow rate for pipe diameters greater than 0.02m. This is an important finding because it gives credibility to the assumptions that frictional resistance can be ignored when modeling large pipelines. The effects of different size discharge conditions were not evaluated in this experimental work. Discharge conditions and sizes have a significant effect on the celerity of air bubbles because of local losses that may be present in these structures.

Benjamin (1968) developed the mathematical model to describe the characteristics of gravity currents in a closed pipe of a square cross-section. He argued that in horizontal pipes, the gravity current flow, is horizontal far downstream and the cavity and fluid each fill up to 50% of the space in the pipe. This finding has been confirmed by subsequent studies by Baines (1991) and Weber and ME (1981). When the conditions are conducive for gravity current flows, then the is a balance between hydrostatic forces and hydrodynamic drag which results in the elimination of energy dissipation in the flow leading to a constant air bubble celerity through the pipe. In a horizontal pipe, the air cavity has different flow zones as demonstrated in Figure 2.2

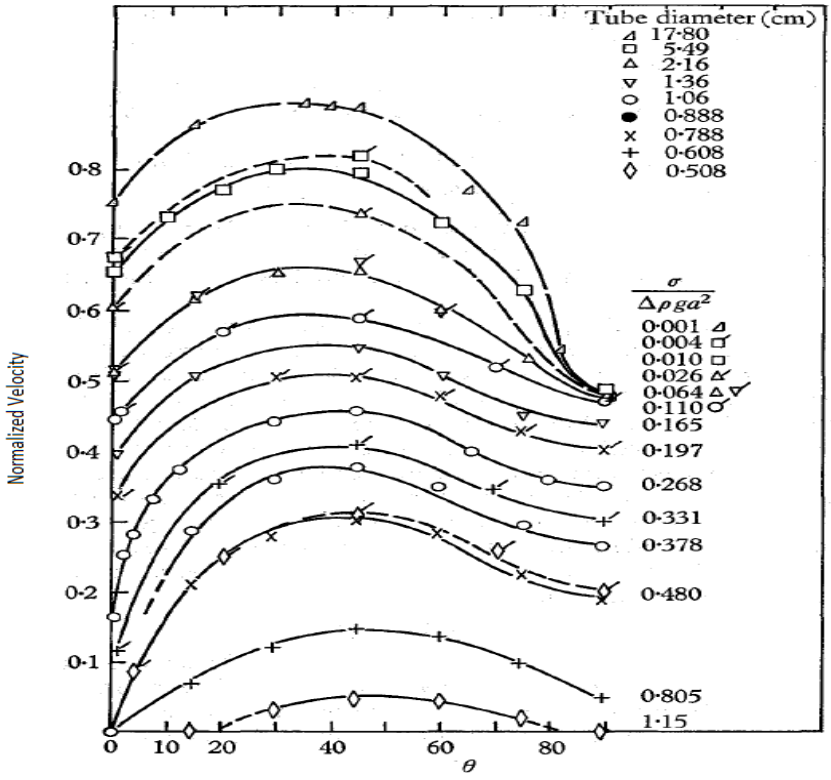

Figure 2. 1 Effects of pipe angle of inclination in the gravity current velocity. (Zukoski, 1966)

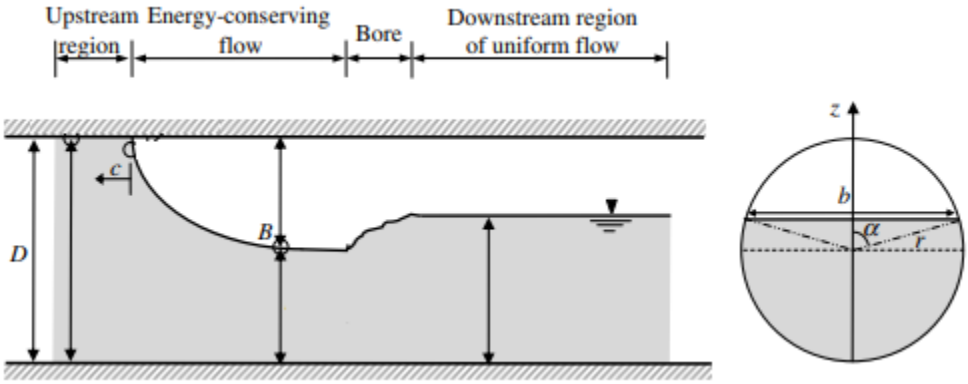

Figure 2. 2 Different zones of gravity flow in a horizontal pipe (Bashiri-Atrabi et al. 2016)

Zukoski (1966) and Benjamin (1968) concluded that

- The flow rate is influenced by the ratio of liquid height in the pipe divided by the diameter of the pipe
- They found the celerity to be between

$$\boldsymbol{c = 0.767 * \sqrt{gD}} \qquad \text{Equation 2.1}$$

And

$$\boldsymbol{c = 0.47 * \sqrt{gD}} \qquad \text{Equation 2.2}$$

- The fluid height in a horizontal gravity current can't be less than half the pipe diameter
- The velocity of the air cavity was shown to be faster in circular pipes than square pipes

The celerity was found to be proportional to the Froude number, with the constant of proportionality depending equal to 0.542 which however has been found to be theoretical value than a practical valve.

Baines (1991) conducted his experiments on a square pipe to study how the gravity current or cavity formed by the sudden opening of the discharge port, propagates and shapes as it travels through an inclined pipe. The discharge port was characterized by a weir which would be opened to different heights namely, 0.25H, 0.5H, 0.75H, and H, where H is the pipe height. The pipe slopes were varied between 0 degrees and 8 degrees.

The momentum equation was used with the continuity equation to show the cavity propagation through the square pipe. These equations were manipulated to get the below equations, equation 2.3 and 2.4:

$$\frac{1}{2}(p_A + p_E)H - \frac{1}{2}(p_c + p_D)y_f + W sin\theta = \rho q(V - V_f) \quad \text{Equation 2.3}$$

$$V_f^2\left(\frac{H}{y_f} - \frac{1}{2}\right) = V_{f0}^2\left\{2\, cos\theta\left[1 - \left(\frac{y_f}{H}\right)^2\right] + 4\, I\, Sin\theta\right\} \quad \text{Equation 2.4}$$

Where P_A, is the pressure at A, W is the weight of water in between 1 and 2 in Figure 2.3 and q = unit discharge, I is the cross-sectional area of water under the front, V_f is the front velocity. y_f = h/2.

Alves et al. (1993), added to the study of gravity currents by modifying the Benjamin (1968) theory to include inclined circular pipes and added surface tension effects on gravity currents. They conducted experiments on inclined and horizontal pipes and vertical pipes. In their experimental work, they used kerosene as the liquid fluid with capacitance sensors and pressure transducers to measure the instantaneous liquid holdup and pressure differential, respectively. A predetermined volume of air was released to a stagnant volume of water and the velocity of the air volume was measured by the capacitance sensors. They noted that since the hydraulic head for inclined pipes is greater than the radius of the pipe, the flow rate would be greater. The Benjamin (1968) theorem for calculating gravity current was modified as presented below, from equation 2.5. In his theorem Benjamin (1968) used a control frame that moves with the velocity of the bubble such that the movement of the cavity is always at a steady-state, refer to Figure 2.3

Fom the continuity equation:

$$AV_1 = AV_2 \qquad \text{Equation 2.5}$$

And Bernoulli equation from points 1 to 2 taking to account the effects of surface tension such that the is a pressure difference between point 0 and inside the bubble:

$$\frac{P_1}{\rho} + \frac{v_1^2}{2} + xgsin\beta = -\frac{\Delta P_{\sigma 0}}{\rho} \qquad \text{Equation 2.6}$$

Bernoulli equation between points 0 and 2 along the free surface

$$\frac{v_2^2}{2} - g[ysin\beta + (D-h)cos\beta] = -\frac{\Delta P_{\sigma 0}}{\rho} + \frac{\Delta P_{\sigma 2}}{\rho} \qquad \text{Equation 2.7}$$

$\Delta P_{\sigma 0}$ *pressure difference between stagnation point and pressure inside bubble*

Assuming that momentum is preserved between points 1 and 2

$$\left(P_1 + \frac{1}{2}\rho g D\, cos\beta\right)A + \left[xA + \int_0^y A_2 dy\right]\rho g sin\beta \qquad \text{Equation 2.8}$$

$$-\cos\beta \int_0^h \rho g(h-z)b\, dz - P_2A_2 = \rho v_2 A_2 (v_2 - v_1)$$

From Figure 2.3,

$$y = cos^{-1}\left(2\frac{h}{D} - 1\right)$$ Equation 2.9

$$A_2 = \left(\pi - y + \frac{1}{2}\sin 2y\right) r^2$$ Equation 2.10

$$\int_0^h \rho g(h-z) b\, dz = r\left(A_2 \cos y + \frac{2}{3} r^2 sin^3 y\right)$$ Equation 2.11

Substituting P_1 from equation 2.5 and v_1 from equation 2.6, V_2 from equation 2.7and equation 2.11 into equation 2.8

$$\left[A_2' y' - 2A_2' y' + \int_0^{y'} A_2'\, dy'\right] tan\beta - A_2'(2 - A_2')(1 - h') + \frac{1}{2} -$$ Equation 2.12

$$\frac{1}{2}\left[A_2' \cos y + \frac{2}{3\pi} sin^3 y\right] - \frac{(A_2' - 1)^2 \Delta P_{\sigma 0}'}{cos\beta} + \frac{(A_2' - 1) A_2' \Delta P_{\sigma 2}'}{cos\beta} = 0$$

Where $y' = y/D$, $h' = h/D$, $A_2' = A_2/A$

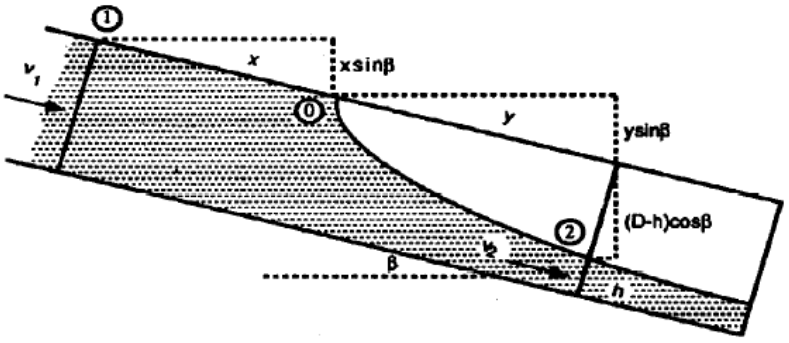

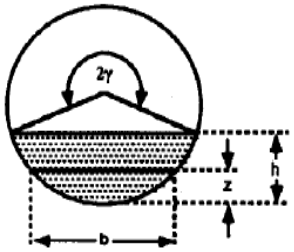

Figure 2. 3. Schematic drawing of the model. (Alves et al. 1993)

After some simplifications, Figure 2.4 can be plotted by assuming an elliptical shape for the flow bubble and ignoring small values for y' since equations 2.4 and 2.6 only apply to uniform flows. The authors then proposed the following expression combining equations 2.5 and 2.7:

$$\frac{u_d}{\sqrt{gD}} = \frac{v_1}{\sqrt{gD}} = (1-\xi)\, x \sqrt{2[y' \sin\beta + (1-h')cos\beta - \Delta P'_{\sigma 0} + \Delta P'_{\sigma 2}]} \qquad \text{Equation 2.13}$$

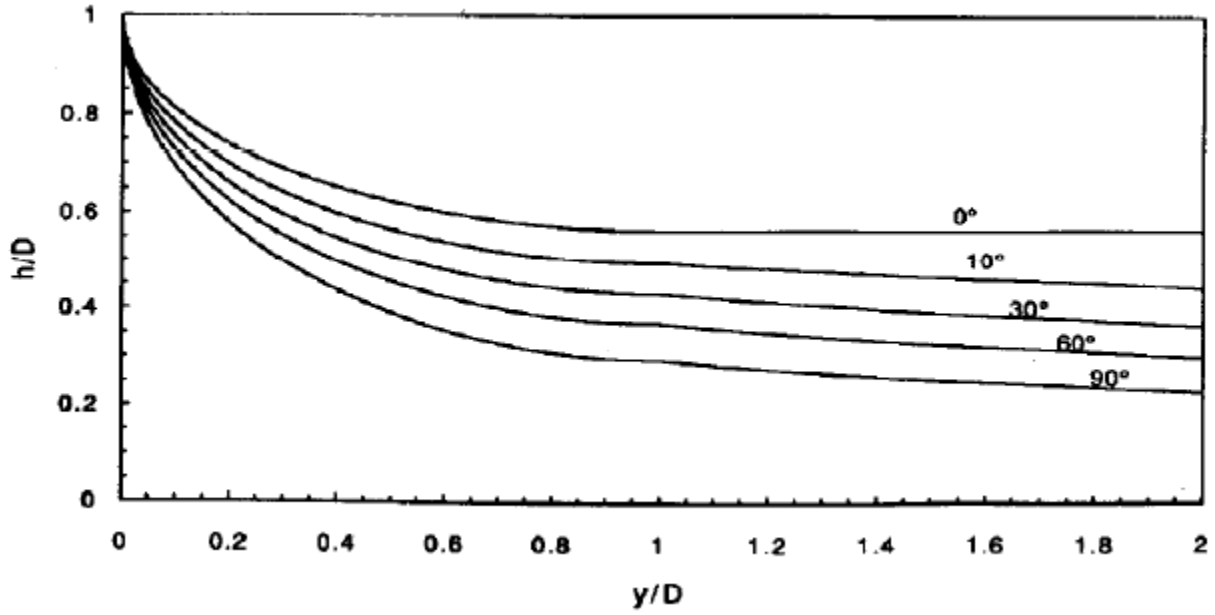

Figure 2. 4. Predicted gravity current for inclined pipes (Alves et al. 1993)

Alves et al. (1993) compared the results of their theory and experiments with that of Benjamin (1968) and Zukoski (1966) and found that:

- Experimental data was different from theoretical predictions for the horizontal case, theoretical data predicted $\frac{u_d}{\sqrt{gD}}$ = 0.54 while experimental data showed $\frac{u_d}{\sqrt{gD}}$ = 0.47
- The was good agreement between the theoretical and horizontal data for inclined conditions.
- The model predicted lower values for $\frac{u_d}{\sqrt{gD}}$ than those presented by Zukoski (1966) for inclined pipe
- The model showed similar values for $\frac{u_d}{\sqrt{gD}}$ to those presented by Zukoski (1966) for the horizontal case
- The celerity of the bubble was found to increase with decreasing slope, from 90 degrees to 45 degrees, a finding consistent with that of Zukoski (1966)

In their experimental work, Alves et al. (1993) introduced a bubble on known volume into the pipe. This is not always representative of real-world conditions where an infinite volume of air can be introduced into the pipe. Figure 2.4 which was used as a basis for calculating the bubble velocity was developed using estimates and assumptions (especially for smaller slopes), which is probably the reason their results were not exact with those of Zukoski (1966).

2.1.2 Gulping

Gulping is the phenomenon also known as glug-glug, according to Clanet and Searby (2004) it is the oscillatory emptying of a pipe. This behavior is observed when a liquid is emptying under conditions where the discharge orifice is less than half the diameter of the emptying pipe. Clanet and Searby (2004) further states that the gulping is caused by a succession of discharge jets of the water (liquid) closely flowed by the intake of air bubbles into the pipe. Geiger et al. (2012) observed that there were two types of gulping, for small diameters, where the discharge orifice to pipe ratio is less than 0.25. For this case, the is oscillatory flows whereby there is a liquid escape followed by gas intake and re-pressurization and refill. For discharge orifice to pipe diameter ratio closer to 0.5, then gulping is characterized by simultaneous inflow and outflow where the water leaves the pipe adjacent to the pipe walls and air (bubbles) are introduced in the middle. This shows that the exchange of water leaving the pipe and air entering the pipe can be simultaneous or in turns depending on the discharge orifice diameter to pipe ratio.

Kordestani and Kubie (1996) conducted investigations into the phenomenon of gulping using a vertical pipe. Two experiments were conducted, in experiment one, water was used as the liquid fluid discharging to air while in experiment two, water discharged to paraffin. The investigation was conducted to find the pressure variations inside a closed bottle as liquid is drained into the air or liquid is drained to another liquid of less density. The diameters of the outlet orifice were varied for the different experiments. Air pressure was measured at the top of the pipe.

Using Figure 2.5, Kordestani and Kubie (1996) proposed the following relationship between diamter of pipe and diameter of orifice

$$C = 0.55 + 0.044\frac{D_v}{D} - 0.0013\left(\frac{D_v}{D}\right)^2 \quad \text{Equation 2.14}$$

$$C = 0.78 + 0.046\frac{D_v}{D} - 0.0015\left(\frac{D_v}{D}\right)^2 \quad \text{Equation 2.15}$$

Where *Dv* is the pipe diameter and *D* is the outlet diameter.

Equation 2.14 is for $\left(\frac{D_v}{D}\right)$ less than 0.25 while equation 2.15 is for $\left(\frac{D_v}{D}\right)$ between 0.25 and 0.5

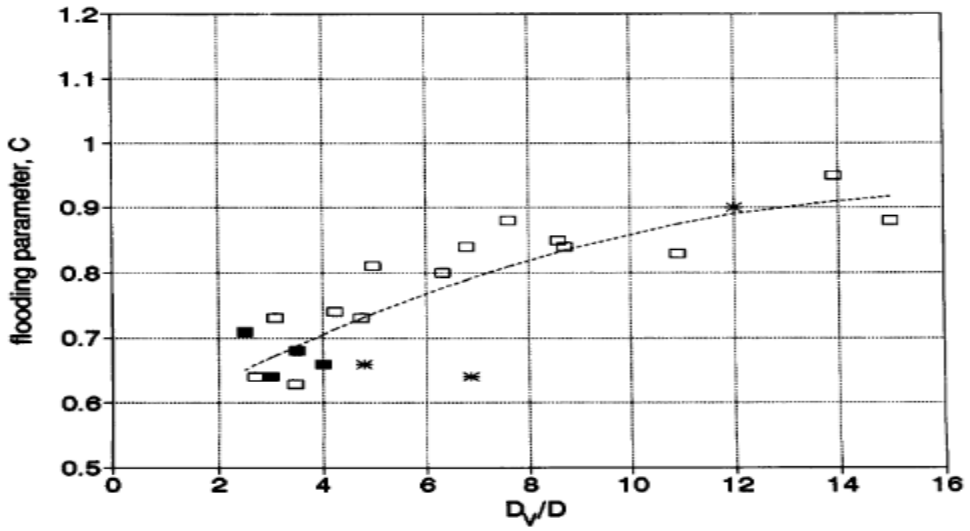

Figure 2. 5. A plot of flooding parameter, C, with respect to the diameter of discharge orifice and pipe diameter (Kordestani and Kubie, 1996)

Kordestani and Kubie (1996), found that:

- The level of water in a pipe without ventilation does not influence the hydrostatic pressure and the air pressure in the pipe.

- Liquid to liquid discharge properties are like liquid to air discharge, the only difference is that the liquid to liquid discharge has reduced interfacial velocities.
- The discharge port determines the process of discharge and it's independent of pipe height or liquid depth
- The flooding parameter increases with the ratio of discharge port diameter and pipe diameter

Kordestani and Kubie (1996) experimental work did not include inclined pipes.

Clanet and Searby (2004) used a vertical pipe to conduct experiments investigating gulping. The investigation focused on the time taken for the vertical pipe to empty and the oscillation time of the water-air interchange. The experiments were carried out using liquids of different properties and the discharge orifice diameter was varied. They also developed the gulping model using the spring-mass analogy. Euler equations were used to describe the liquid movement inside the pipe. They determined that

- The mass of water inside a pipe closed at the upper-end decreases (almost) linearly with discharge.
- Another important observation was that the oscillations period and magnitude varies with the water height in the pipe.
- The initial pressure drop when the downstream valve is opened is equal to the height of the water column and increases to atmospheric pressure as more air is introduced into the system.

- The pressure oscillations have a shorter period as compared with the emptying flow rate, which shows that the oscillations are related to the rate at which bubbles are formed at the exit point, not the flow rate.
- The air compressibility plays an important role in the modeling of the gulping. They compared results from models considering air compressibility and other models not considering air compressibility and found that the models with air compressibility yielded results that were closer to experimental data than the models without air compressibility. Ignoring the compressibility of air slows down the flow rate by approximately 35% in this case.

This experimental work only considered vertical pipes. This is a limitation because a change in slope directly affects the angle at which the liquid escapes from the pipe. It is expected that a change in angle results in different governing equations and results.

Geiger et al. (2012) added to the knowledge of gulping by conducting experiments and developing a CFD model to predict the properties of gulping in inclined pipe. Two experiment types were performed, these were; measuring the complete emptying time for a pipe filled with water and the other was measuring the pressure variations at the top of the pipe during the emptying process. The experimental data was compared to the CFD model results

Geiger et al. (2012), found that

- The emptying time is reduced as the diameter of the discharge port is increased. This is due to the bigger discharge port allowing a greater volume of water to escape from the pipe.

There was however no clear correlation between the discharge orifice size and discharge time.

- For orifice sizes equal and less than half the pipe diameter, and oscillatory flow pattern was observed, while for discharge port larger than half the orifice size, counter flows were observed. The effects of inclination on the flow pattern were found to be that where gulping occurs, mild slopes increase lead to upsurge in the outflow rate (slopes between 45 and 30 degrees) while for counter flows, the reverse is true, an increase in slope leads to decrease in flow rate.

This research could have been improved by studying the effects of gulping on different diameters and the effects of inclination on the flooding constant, C.

2.2 Pipe emptying investigations

2.2.1 Studying pipe emptying events through numerical modeling

Liou and Hunt (1996) developed a model to predict the water column length, velocity, and pressure changes when filling pipelines with irregular profiles. The model used four major assumptions. These are that the liquid in the pipe has a defined front interface, the pressure at this interface is equivalent to atmospheric. The rigid water column theory was assumed and the model was developed using the frictional low resistance relationship. Pipe filling experiments with constant head water supply were carried out to assess the applicability of the model. The model was found

to have limitations where the is an occurrence of free surface flows and water column separation. The model was developed based on the momentum equation

$$\frac{dQ}{dt} = \left(\frac{P_0}{\rho L} + g\sin\theta - \frac{fV^2}{2D}\right)A \qquad \text{Equation 2. 16}$$

$$L = L_{min} + \int_0^1 V\,dt \qquad \text{Equation 2. 17}$$

The pressure of the pipe immediately downstream of the valve separating the reservoir and pipeline is P_0 and its calculated as

$$P_0 = \rho g\left(H_R - K\frac{V^2}{2g}\right) \qquad \text{Equation 2. 18}$$

Where H_R is found by integrating Euler's equation of motion from the reservoir surface to the pipe inlet

$$H_R = \frac{P_1}{\rho g} + \frac{V_1^2}{2g} + z_1 = \frac{1}{g}\int_1^2 \frac{\partial V}{\partial t} + \frac{P_2}{g} + \frac{V_2^2}{2g} + z_2 \qquad \text{Equation 2.19}$$

Where z and s represent the elevation and streamline distance, respectively.

From Equation 2.19 it can be deduced that the available head to drive flow is reduced by

$$\left(\frac{L_0}{g}\right)\left(\frac{dV}{dt}\right)$$ Equation 2.20

Such that as the local acceleration reduces, the head driving flow increases to H_R. if equation 2.16 is written in term of velocity then,

$$\frac{dV}{dt} = \frac{\frac{g}{L}\left(H_R - K\frac{V^2}{2g}\right) + g\sin\theta - \frac{fV^2}{2D}}{1 + \frac{L_0}{L}}$$ Equation 2.21

$$P_0 = \rho g\left(H_R - \frac{L_0}{g}\frac{dV}{dt} - K\frac{V^2}{2g}\right)$$ Equation 2.22

It was shown by Liou and Hunt (1996) that the rigid column theory can be applied between successive pipe segments by using the final solution of the previous segment and equating it to the initial conditions of the next segment. The model ignored the initial transient behavior of pipe filling.

Izquierdo et al. (1999), improved on the model by Liou and Hunt (1996), by modifying the model to evaluate peak pressure resulting from air-water interactions in pipelines. The model assumptions were that the is a well-defined interface between the air and water, the ideal gas laws apply for the air phase with a polytrophic coefficient of 1.2, and the water acts as a rigid column. In water pipeline filling, the smallest air pocket has the largest pressure peak and the presence of multiple air pockets does not affect the pressure and velocity peaks of the first air pocket.

Trindade and Vasconcelos (2013), developed two models for air-water interactions which were verified by experimental data. These models included ventilation in the analysis. The first model is called the shock-capturing model. It uses the Saint-Venant and Preismann slot method to model the water phase and pressurization, respectively. The second model used the two-component pressure approach to mitigate the limitation of low courant numbers. For the experimental work, the was a systematic variation of flow rate, slope, ventilation, and orifice diameter. The experimental data and modeling results matched well for both models.

Coronado-Hernández et al. (2018) developed a mathematical model to predict the emptying processes in the pipeline using pressurized air. They used the rigid water column theory to predict the pressure changes during the emptying period. This model was compared with the experimental results and found to be accurate. The model they presented is versatile as it can be used with most pipeline configurations with minor modifications. The model combined the mass oscillation equation with interface position as presented below:

$$\frac{dv}{dt} = \frac{p_1}{\rho_w L_e} + g\frac{h_s}{L_e} - f\frac{v|v|}{2D} - k(\theta)\frac{v|v|}{2L_e} \qquad \text{Equation 2.23}$$

And the interface position during the emptying process can be modeled by:

$$\frac{dLe}{dt} = -v \qquad \left(L_e = L_{eo} - \int_0^t v dt\right) \qquad \text{Equation 2.24}$$

Where p_1 is the driving gauge pressure, L_e is the length of the emptying column, h_s length of vertical pipe, v is the water velocity, D internal diameter, $k\ (\theta)$ is the minor loss coefficient and g is the acceleration due to gravity. The model solved a 2 X 2 system of differential equations that were solved using Simulink in MATLAB.

Besharat et al. (2018), developed a one-dimensional model and a two-dimensional CFD model to predict low-pressure conditions as well as the relationship between backflow air and pressure changes in pipe emptying. The model results were compared with experimental results. The experimental data was collected from a pipe with a confined air pocket and the discharge port diameter was varied for different experiments, the smallest opening size was 6% of pipe diameter. The opening of the discharge valve allowed the water to drain therefore causing the air pocket to move and pressure in the air pocket to drop. The one-dimensional model used the rigid water column theory and the air expansion was modeled using a polytrophic expression. The momentum equation 2.24 was used for tracking of the water velocity. The air-water interface was predicted by the piston flow model

$$\frac{dLw}{dt} = -V_w \qquad \text{Equation 2.25}$$

These equations were solved on Simulink in MATLAB. The one-dimensional and two-dimensional CFD models were found to give acceptable results with the one-dimensional model giving slightly better results in the first few seconds of simulation.

Fuertes-Miquel et al. (2019) studied transients in pipe emptying. They improved on the rigid column using oscillatory equations for the pipe emptying model by Coronado-Hernández et al. (2018) by adding ventilation. They studied the emptying process by considering two cases, trapped air without ventilation and ventilated pipe with two orifice sizes. For the modeling of entrapped air, they added the term

$$\boldsymbol{P_1^* V_a^k = P_{1,0}^* V_{a,0}^K \;\; or \; P_1^* x^k = P_{1,0}^* x_0^k} \qquad \text{Equation 2.26}$$

Where Va = air volume, $Va_{,0}$ is the initial air volume, $P^*_{1,0}$ is the initial value of P^*_1, x_o is the initial length of x. therefore instead of a 2x2 system of equations, Fuertes-Miquel et al. (2019), solved a 3x3. The ventilation was modeled by considering continuity such that

$$\boldsymbol{\frac{dm_a}{dt} = \rho_{a,nc} v_{a,nc} A_{adm}} \qquad \text{Equation 2.27}$$

Using the chain rule and the definition of air mass yields:

$$\boldsymbol{\frac{dm_a}{dt} = \frac{d\rho_a V_a}{dt} = \frac{d\rho_a}{dt} V_a + \frac{dV_a}{dt} \rho_a} \qquad \text{Equation 2.28}$$

Where m_a is air mass, $v_{a,nc}$ is the air velocity in normal conditions admitted by ventilation and A_{adm} is the cross-sectional area of the air valve.

If:

$$\boldsymbol{V_a = xA = (L_T - L_e)A \;\; and \; \frac{dVa}{dt} = \left(\frac{-dL_e}{dt}\right) A = \; vA} \qquad \text{Equation 2.29}$$

Then,

$$\frac{d\rho_a}{dt} = \frac{\rho_{a,nc} v_{a,nc} A_{adm} - v_w A \rho_a}{A(L_T - L_e)}$$ Equation 2.30

The expansion-compression equation:

$$\frac{dp_1^*}{dt} = -k \frac{P_1^*}{V_a} \frac{dV_a}{dt} + \frac{P_1^*}{V_a} \frac{k}{\rho_a} \frac{dm_a}{dt}$$ Equation 2.31

The additional equations result in a system of algebraic and ordinary differential equations. The model was found to accurately predict the pressure changes for both the ventilated and unventilated pipes. The bigger ventilation was found to produce smaller pressure changes as compared with the small ventilation. In the case where the was no ventilation, the opening of the gate valve resulted in sub-atmospheric pressures in the system. The results also showed that a sub-atmospheric pressure trough is controlled by the ventilation condition upstream. This study would be improved by studying the effects of changing the discharge orifice size.

2.2.2 Studying pipe emptying events through Experiments

Xue and Zheng (2011) conducted experiments by changing the discharge port sizes to develop a mathematical tool for calculating the discharge volume based on the pressure changes and emptying time. The model was based on the ideal gas law and is useful for long distance pipelines because it allows the pipeline to be analyzed in smaller sections. It was found that the lower discharge flow rates resulted in increased sub-atmospheric pressure conditions. In their study Xue and Zheng (2011) they did not consider the effects of not having an air valve. The absence of air valves presents the biggest challenge to the water system during emptying.

Laanearu et al. (2012) conducted investigations into horizontal pipeline emptying by pressurized air while varying the discharge port conditions. The experiment focused on the advance of the air-water interface. The pressure changes during the emptying process as well as the formation of the interface are tracked. Water was drained from the pipeline while pressurized air was introduced. A control volume numerical model was developed to explain the observed results. As the pipeline drained the air pressure reduced and a horizontally stratified air-water interface was formed. A mathematical model was developed using the conservation of momentum refer to Figure 2.6

$$\frac{dV}{dt} - g\frac{(h_p - h_f)}{L} = \beta\left(\frac{1}{\alpha} - 1\right)\frac{U^2}{L} - \frac{U^2}{L} \qquad \text{Equation 2.32}$$

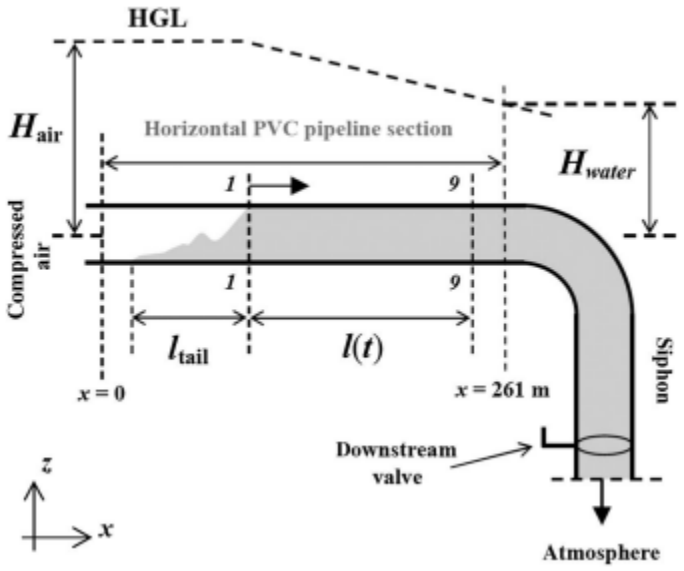

Figure 2. 6 Control volume model sketch (Laanearu et al., 2012)

Where h_f is the Darcy-Weisbach friction head loss, h_p is the pressure head difference. L_{tail} is the tailing water behind the air front head. β is the correction factor for momentum changes as the water and air move inside the pipe. In this study, only the horizontal case was considered. This study could have been improved by including a comparison of a pipe draining under gravity and pressurized air.

Bashiri-Atrabi et al. (2016) and Mer et al. (2018), carried out experiments to investigate the air interference in horizontal and inclined circular pipes. The experimental data were compared with modeling data for interface tracking using the hydrostatic pressure model and using the Boussinesq model to predict the water surface profile. The experiments were performed using a transparent pipe with an adjustable weir at the discharge outlet. The hydrostatic model was developed from the Saint-Venant equations consisting of continuity and momentum equations as follows:

$$\frac{\partial A}{\partial t}+\frac{\partial Q}{\partial x}=0 \qquad \text{Equation 2.33}$$

$$\frac{\partial A}{\partial t}+\frac{\partial Q}{\partial x}+gA\cos\theta\frac{\partial h}{\partial x}=gA\left(\sin\theta-\frac{\tau_{bx}}{\rho gR}\right)+\frac{\partial(-\overline{u'^2}A)}{\partial x} \qquad \text{Equation 2.34}$$

The pressurized zone is represented by

$$\frac{\partial Q}{\partial x}=0 \qquad \text{Equation 2.35}$$

$$\frac{\partial A}{\partial t}+\frac{\partial Q}{\partial x}+gA\frac{\partial}{\partial x}\left(\frac{P_D}{\rho g}+D\cos\theta\right)=gA\left(\sin\theta-\frac{\tau_{bx}}{\rho gR}\right)+\frac{\partial(-\overline{u'^2}A)}{\partial x} \qquad \text{Equation 2.36}$$

Where τ_{bx} is the wall shear stress and $-\overline{u'^2}$ is the turbulence intensity while P_D is the pressure on top of the pipe. It was presented that the cavity intrusion has three distinct zones as shown in Figure 2.7. The conclusions from this experimental work showed that the flow out of a pipe depended on the downstream conditions The pressure drop equivalent to the air pressure drop was noted at the stagnant liquid which suggests that when the emptying process starts, sub-atmospheric pressure is introduced throughout the pipe system.

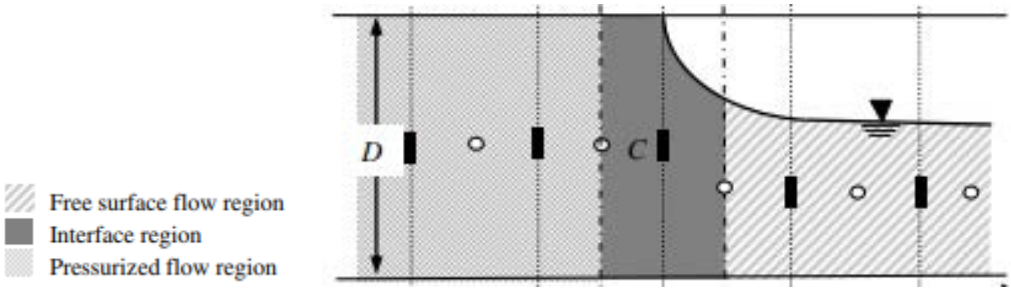

Figure 2. 7. Three cavity zones as defined by Bashiri-Atrabi et al. (2016)

Bashiri-Atrabi et al. (2016) concluded that the downstream conditions of the pipe determined the water flow profile Fuertes-Miquel et al. (2019) concluded that the upstream end determined the flow surface profile. Therefore both the upstream and downstream can be controlling agents in pipe emptying. This is determined by the characteristics and conditions of the pipe flow. Ventilation upstream of the pipe was not considered in this study and this might have led to the conclusion that downstream conditions control the pipe flow. In Fuertes-Miquel et al. (2019) ventilation upstream was considered. This shows that there is a transition point where the flow is

either controlled upstream or downstream when the is ventilation and different orifice discharge sizes.

Coronado-Hernández et al. (2017) studied the pipe emptying process for conditions where there is an irregular pipe profile and multiple air valves and multiple discharge points, as shown in Figure 2.8. A one-dimensional rigid theory model was developed and used to model this system. The experiments were carried out on a pipe system with angels of 30 degrees to the horizontal with air valves installed at the apex of these pipes. The model used the rigid column theory and mass oscillation equations, only that here they were applied in successive emptying columns. It was concluded that

- The size of the air pocket determined the value of the sub-atmospheric pressure. Smaller air pockets resulted in lower sub-atmospheric pressure.
- The model was accurate in predicting the evolution of air pressures and water velocity.

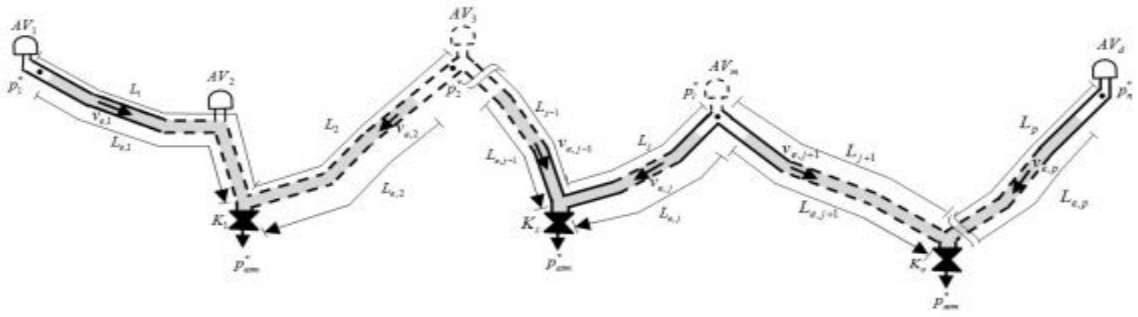

Figure 2. 8 Irregular pipe profile with multiple discharge and ventilation points (Coronado-Hernández et al. 2017)

The research ignored the effects of discharge conditions on the pressure and flow rates of the emptying system. The discharge conditions, size, or shape can greatly affect the pressure and flow rates.

2.3 Pipe ventilation

Zhou et al. (2002) studied the effects of ventilation size on pressure variation in filling of horizontal pipes. The investigation was both numerically and experimentally. The experiment was conducted on a horizontal pipe connected to a reservoir and an orifice was placed extreme downstream side of the pipe. Different water column lengths and orifice sizes were used. The orifice sizes were classified as a ratio of d/D with less than 0.086 representing the type 1, type 2 was represented by orifice size between 0.086 and 0.2 while type 3 was represented by orifice size greater than 0.2. For the numerical investigation, momentum equation was used as shown

$$\frac{dV}{dt} = -g\frac{H - H_0}{x} - f\frac{U|U|}{2D} - \frac{U^2}{2x} \qquad \text{Equation 2.37}$$

While the change in the volume of air in the horizontal pipe was given by

$$\frac{dV_a}{dt} = -AV \qquad \text{Equation 2.38}$$

The governing equation for the air phase was given by,

$$\frac{dH^*}{dt} = -k\frac{H^*}{V_a}\frac{dV_a}{dt} - k\frac{H^*}{V_a}Q_a \qquad \text{Equation 2.39}$$

Where Q_a is the flow rate from the orifice given as

$$Q_a = C_d A_0 Y \sqrt{2g \frac{\rho_w}{\rho_a} (H^* - H_b^*)}$$

Equation 2.40

Zhou et al, (2002) found that the type 1 orifice size resulted in reduced pressure, the air, in this case, acts as a sponge to absorb the pressure effect from the hydraulic head provided by the reservoir. Type 3 orifice resulted in high pressure. The experimental data were compared with the numerical model and found to be accurate. This study could be improved by adding an inclined pipelines.

Balacco et al. (2015), conducted experiments to investigate the effects of ventilation orifice size, pipe slope, and discharge orifice size on pressure and flow rates in pipe filling. The experimental setup had the ventilation orifice at the top of two adjoining pipes and had a constant water head supply. The angle of inclination had a major influence on the air pressure inside the pipe. An increase in pipe slope resulted in greater peak air pressure. The size of the water discharge port was significant in pressure variation. When 50% of discharge valve was opened it produced larger peak pressures for the same ventilation sizes. The maximum peak pressures were observed with the discharge valve fully closed. The ventilation size was found to have no significant effect on the peak pressures for steep slope and partially opened discharge valve.

Li et al. (2018) improved on the work of Zhou et al. (2002) by changing the orifice position from the end of the pipe to the top and at different locations along the pipe. They also varied the orifice sizes and used a 3D CFD model to simulate the pressure changes. The analytical model assumed

that water acts as a rigid column, the polytropic law governs the air phase, the filling process is characterized by a vertical air-water interface. It was concluded from this research that for the cases where the is no leakage allowed, the peak pressure is maximum and lowest for cases where the is maximum leakage. The magnitude of the water hammer also depended on the leakage orifice size, the bigger the orifice the smaller the magnitude of the water hammer pressure. When the air leakage is towards the end and on top of the pipe, the oscillation period is dependant on the driving pressure and length of entrapped air. This study could have been improved by including inclined pipes.

Fuertes-Miquel et al. (2019) conducted experiments to study air valves in water systems to develop a numerical model to show maximum pressure changes. The experiments considered different cases of ventilation size, length of the water column, and period it takes for the valve to open. The numerical model was developed with the assumptions of the rigid column model used together with the mass oscillation equation. From their experiments, it was found that the sizing of air valves was critical to avoiding dangerous situations. Smaller air valves can result in excessive compression of air pockets in the pipe while large air valves can lead to water hammer. Isothermal assumptions in modeling resulted in greater air pocket pressure than adiabatic assumptions.

2.4 Slug-flows

Nicholson et al. (1978) developed on Benjamin (1968) and studied intermittent two-phase flows. These can be described as two-phase flow where the elongated bubble also has slug flows. Slug

flows is the region of liquid flow found in between gas bubbles. Figure 2.9 shows the different flow zones in slug flows.

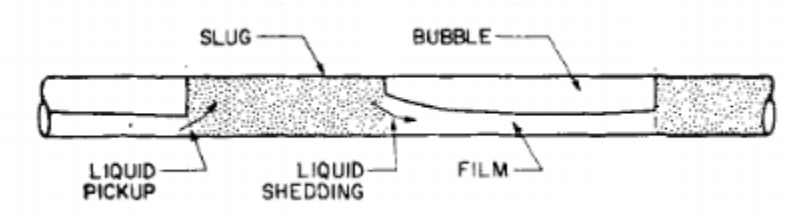

Figure 2. 9. The intermittent flow regime in slug flow (Nicholson et al. 1978)

For horizontal pipes two-phase flow can be divided into three, namely;

i) Elongated bubble – this is the main part of the flow, like the bubble described by Benjamin (1968).
ii) Elongated bubble flow with dispersed bubbles – this is a combination of the main bubble with smaller bubbles with may or may not be attached to it
iii) Slug flow – the flow regions between gas bubbles (Bendiksen, 1984)

Bendiksen (1984), conducted an experimental investigation of the movement of elongated cavities in inclined pipes. The experiment involved the introduction of a bubble into a liquid that is flowing at a certain velocity. The tests were done over a range of inclinations from -30 degrees to 90 degrees. The results for low liquid velocities, the results were close to stagnant liquid flows cavity propagation. As the liquid velocity was increased, the cavity celerity decreased. For cases where the angle was less than 0 degrees, it was found that the induced cavity will at some critical point

turn and propagate faster than the liquid. There wasn't a good correlation of data for this experimental work with other experiments. This was caused by the discrepancy in results and data presented from experiments with inclined pipes.

Weber et al. (1986), studied the velocity of bubbles in a vertical, horizontal, and inclined pipe. The angles of inclination were from 15 degrees to 75 degrees at 15-degree increments. It was found that the bubble length had no effect on the bubble velocity and that as the pipe drained the bubble had constant velocity and shape. The bubble velocity was shown to be sensitive to the angle of inclination for near-horizontal slopes. The maximum velocity was found at the angle of inclination between 30 and 60 degrees. Only slopes 15 degrees and greater were considered in this research and yet one of the findings was that the inclination angle near the horizontal effects had a marked effect on the bubble velocity. It was recommended to study smaller slopes, less than 15 degrees.

McQuillan and Whalley (1985), noted that the velocity of bubbles in a stationary liquid can also be approximated using the continuity where:

$$\boldsymbol{V_B = C_u V_M + V_D} \qquad \text{Equation 2.41}$$

Where V_B is the velocity of individual gas bubbles in a cylinder with mixed gas and liquid, V_M is a linear function for the whole mixture, total volume divided by the cross-sectional area and V_D is the drift velocity. McQuillan and Whalley (1985) noted that Equation 2.40 has been shown to give consistent results for both vertical and horizontal flows. For horizontal pipes, Equation 2.40 works

well for both elongated bubbles and slug flows. The authors used an earlier study by Gregory and Scott (1969) who presented the slug velocity as the sum of the liquid and gas superficial velocities.

$$\boldsymbol{V_{ns} = V_L^0 + V_G^0} \qquad \text{Equation 2.42}$$

Which gives the relationship between the celerity as and V_{ns} as

$$\boldsymbol{c = 1.35 V_{ns}} \qquad \text{Equation 2.43}$$

The description of two-phase flows is dependent on the flow rates of both liquids, the physical properties of the liquids, and also on the angle of inclination of the pipe. McQuillan and Whalley (1985) separated the vertical two-phase flows into four distinct categories as listed below and shown in Figure 2.10

i) Bubble flow. This is when the water in the pipe flows with visible bubbles which appear as distorted spheres

ii) Plug flow. Plug flow occurs when the is a very high concentration of bubbles in the pipe. These results in the bubbles merging to form bigger bubbles that have the same diameter as the pipe in which they are flowing. The merged bubbles are called plug bubbles because they are shaped like a bullet with a clear leading head and straight back. The plug bubbles appear to be equal diameter as the pipe, but they are surrounded by a thin layer of liquid.

iii) Churn flow. The churn flow is highly irregular characterized by the oscillatory movements of the liquid. This is when the plug flow gets narrower as it follows towards

the exit. Another distinguishing feature is when the slug region in the flow is swallowed by the gas regions and the thin layer of fluid visible in plug flow disappears.

iv) Annular flow. In annular flow, the fluid flows on the walls of the pipe while the gas flows in the middle of the pipe. The fluid also appears in the center of the gas flows

From these descriptions, it can be noted that the different categories of two-phase flows can exist at different stages during pipe emptying. It, therefore, follows naturally that the must be transitional conditions where the flow changes from one type of flow to the next. Bubble flows exit when the is far less gas in the fluid as compared with the fluid. The bubble flow is most likely to transition to plug flow as more gas is added to the pipe.

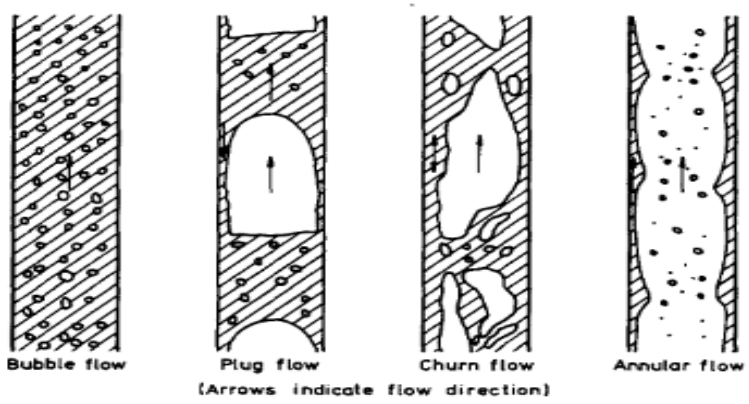

Figure 2. 10 Showing the four regions of flow in for two-phase flows in vertical pipes (McQuillan and Whalley, 1985)

Chapter 3

Knowledge gap and Objectives

There is a wide range of practical issues that involve two-phase flows during pipe emptying operations in the context of drinking water systems. Previous research evaluated the problems of gravity currents, which involved the emptying of pipelines with the focus on the advance of a single gravity current front, and no other ventilation in the system. Other contributions also considered sloped pipes and ventilation, including the numerical modeling of these flows. These studies have not focused on the description of air-water interfaces, thus some of the assumptions used in the development of numerical models were not tested for a wide range of emptying conditions. Different knowledge gaps still exist in the current research, such as:

- For horizontal pipes, would the sub-atmospheric conditions ahead of a gravity current front lead to secondary gravity currents if ventilation were available?
- For sloped pipes, would ventilation prevent the development and advance of gravity currents if unobstructed discharge conditions existed?
- What is the magnitude of flow rate variation over time during emptying processes, and how this depends on ventilation and slope conditions?
- What is the magnitude of pressure variation over time during emptying operation, and how this depends on ventilation and slope conditions?
- Given the different types of air-water interfaces that can appear in emptying processes, what is the ability of numerical models to describe such emptying conditions?

The objective of this research is to study systematically the effect of different variables that have been shown to influence the emptying of pipelines, namely: slope, ventilation, and discharge conditions. These variables affect the behavior of two-phase flows and air-water interfaces, internal pressures, and outflow rates. Another objective of this study is to develop an easy to use tool (created with (VBA), Visual Basic for Applications within Microsoft Excel), to model flow rates and pressures during emptying operations for certain operational conditions. The outcome of this study is to improve our understanding of such flows and assess the applicability of numerical models to describe pipeline emptying operations.

Chapter 4

Methodology

This chapter presents a description of this research methodology, including a discussion of the experimental apparatus, monitoring instruments, and experimental approach used to carry out the pipe emptying investigations. Details are provided here for both the experimental data collection and the numerical model development.

4.1 Experimental program

The experiments were conducted in the Ramsay Hall Hydraulics Laboratory, and a total of sixty (60) different experimental cases were investigated which each test repeated a minimum three times. The experimental cases were varied by:

- The angle of the pipe to the horizontal, a total of 4 slopes, (0, 2.5, 5, 10 degrees with the horizontal),
- The discharge orifice a total of 3 orifice sizes (50 mm, 25 mm and 12.7 mm),
- The area of the ventilation orifice as a percentage of the orifice area to pipe cross-sectional a total of 5 orifice sizes (0%, 0.5%, 1%, 2%, and 3.5% of the pipe cross-sectional area).

4.1.1 Experimental apparatus

The experimental portion of the investigation into pipe emptying required an apparatus set up that would include the essential features of an emptying pipeline. Figure 4.1 presents a sketch and a photo of the apparatus used in the experiments.

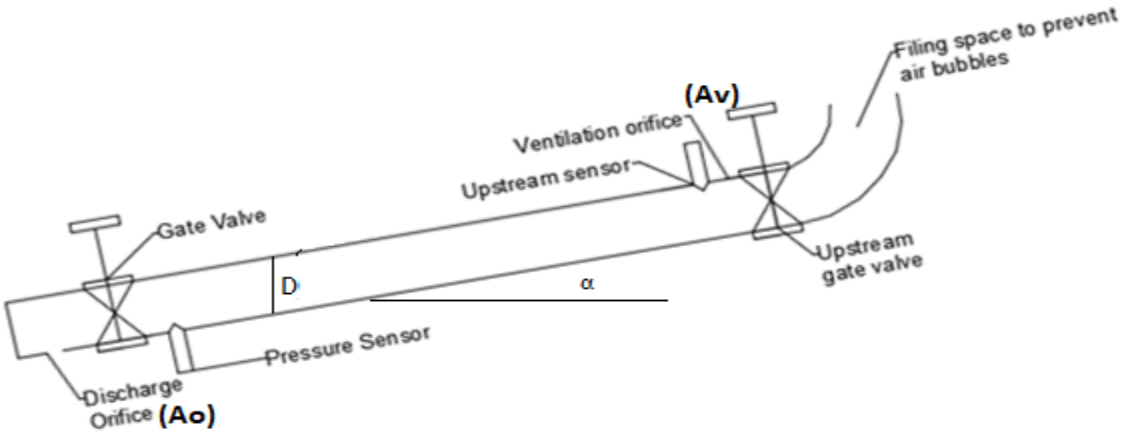

Figure 4. 1 - Top: Apparatus sketch, with a clear PVC pipe with a length of 4.6 m and a diameter of 50 mm. Bottom: Photograph of the apparatus.

The apparatus was fitted with a knife gate valve at the downstream and upstream ends and optionally with a short pipe segment with a cap fitted and two different discharge orifices. When conditions involved a full discharge, the pipe segment with orifice was removed and replaced by a 50-mm elbow directing the water discharge downward as shown in Figure 4.2. When the discharge was restricted, the short pipe segment was maintained, and a preselected discharge orifice was opened. In either case, the emptying starting with the quick opening (~0.3 seconds) of the knife gate valve. Ventilation, when provided, was placed at the crown of the pipe at the upstream end, approximately 5 cm distant from the pressure sensor location.

Figure 4. 2. Experimental conditions of $A_o^* = 1.0$ for the discharge opening

4.1.2 Experimental measurements and instruments

The complete list of experimental instruments includes:

1. Two piezo-resistive pressure sensors (GE UNIK 5000, accuracy range -3.5 to 3.5 m), the accuracy of 0.04%, sampling at 200 Hz.
2. Data Acquisition System (NI USB – 6210, National Instruments) with regulated DC Power supply
3. Digital slope measurement level

4. Two video cameras, recording with a resolution of 1080p, at 30 frames per second

The pipe was fitted with pressure sensors placed at the upstream and downstream of the pipe. The upstream pressure sensor was placed on the pipe crown at 5 cm from the upstream end of the pipe, to capture the local pressure changes, particularly air phase when ventilation conditions existed. The downstream pressure sensor was placed at the bottom of the pipe. These holes were plugged with caulk and tape to ensure that air does not enter the pipe when they are not in use. Table 4.1.

Table 4. 1. Location of sensors and ventilation orifices in the experimental apparatus

Sensor	Location
Upstream piezo-resistive pressure sensor	At pipe invert, 5 cm from the downstream end of the pipe
Downstream piezo-resistive pressure sensor	At pipe crown, 2 cm from the upstream end of the pipe

The pressure measurements were carried out using a GE UNIK 5000 piezo-resistive pressure transducers, connected to the data acquisition system from National Instruments, model NI USB-6210, analog input, and power supply. The sensors used are the piezo-resistive pressure transducers. When connected to the power supply, the sensor receives a voltage, which was carefully kept at 10 volts. When the sensor experiences a change in pressure the strain gage deflects giving off a voltage and this is measured through the data acquisition system connected to a

computer and correlated with measured pressures. The pressure data were collected at 200Hz with an accuracy of 0.04% translating to pressure head accuracy of 0.003 m.

The voltage change measured through the sensors was converted to pressure utilizing the linear relationship between voltage and pressure enabling the calibration of the sensors. A 2-m pipe was used to calibrate the sensors. A sensor was connected at the bottom of the pipe and a known pressure head added to the pipe and sensor measurement recorded. This was done at 30 cm increments and the data plotted in excel and a linear trend line fitted as presented in Figure 4.3.

The flow rate was measured by collecting the volume of water over time. A 102-mm diameter pipe was fitted with one of the piezo-resistive pressure transducers at the bottom. Water was allowed to flow into this pipe and the voltage change as the water rises on the pipe recorded. The pressure increase was plotted on MS Excel, a polynomial fit trend line fitted, and the resulting equation used to calculate the pressure head difference per second. The continuity equation was used to convert the pressure to flow rates. The pressure head was multiplied by the cross-sectional area of the pipe to get the flow rate.

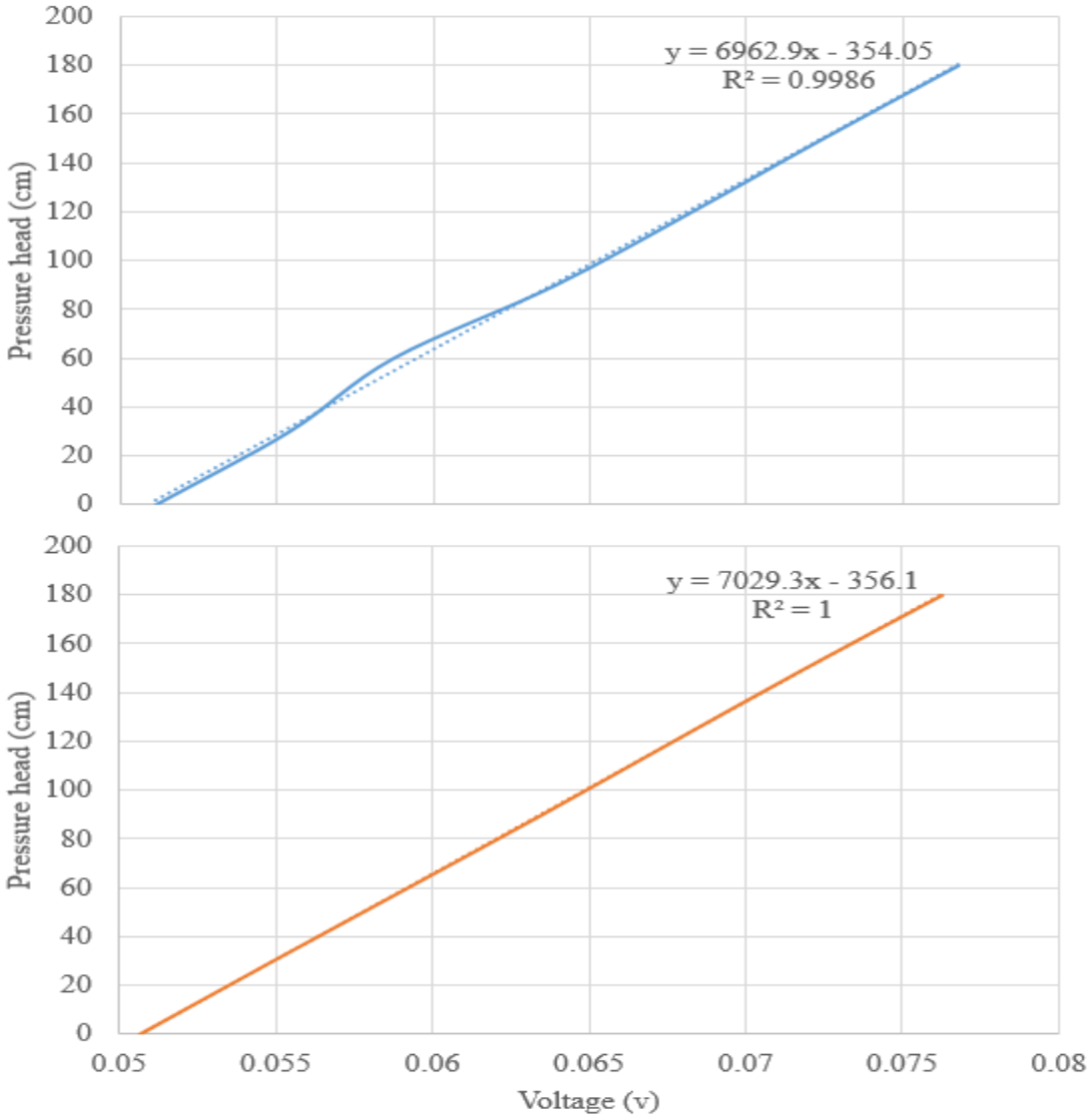

Figure 4. 3. Calibration of pressure sensors

The subsequent equations were used for converting the voltage to pressure

- Sensor 1 equation: H1(cm) = 6962.9 (V) – 354.05

- Sensor 2 equation: H2(cm) = 7029.3 (V) – 356.10; sensor where (V) is the voltage.

The air-water interface was monitored utilizing two video cameras. These were placed as pre-selected locations to capture the entire pipe. Camera 1 was placed to be able to capture the upstream side while camera 2 was placed to capture the downstream side of the apparatus. The videos were recorded and analyzed using the (WMM) Windows Movie Maker software. Given that the pipeline material was clear PVC, black tape markers spaced every 0.30 m in were used to characterize the shape and track the location of the air-water interface(s) over time.

Regarding the filling process before the emptying experiments, care had to be taken to ensure smooth filling to avoid the creation of air bubbles. The air bubbles would have caused inaccurate pressure readings, especially in the upstream pressure sensor. The pipe was lifted and filled from the upstream end through the 90˚ elbow to the brim of the elbow. The angle was made to eliminate the development of air bubbles within the pipe as well as mitigate the presence of air stuck at the upstream side before the experiment starts. The downstream gate valve remained closed the entire filling process. The filling flow rate was controlled through a water tap setup. Slow filling rates were favored because these resulted in laminar flow into the pipe and therefore mitigated the development of air bubbles which would have resulted from turbulent flows into the pipe.

4.1.3 Experimental procedure

1. Adjust the pipeline slope
2. Select desired discharge port and ensure its closed, select desired ventilation
3. For zero slope, raise the upstream side for filling exercise

4. Gradually fill the pipeline to avoid air bubbles
5. For no ventilation, open $A_v^* = 0.035$ to release any air in the pipe system
6. Fill to the top of the 90-degree elbow allowing water to escape through the ventilation
7. Close 90-degree elbow valve
8. Start the cameras
9. Voice record the experimental condition being investigated
10. Start the computer data acquisition recording
11. Initiate flow

The data was collected through a data acquisition board and transferred to a computer via DASQ software

4.1.4 Experimental variables and normalization

Ventilation area (A_v) – a total of five ventilation conditions were considered for the investigation. The ventilation orifice diameters ranged from 3.59 mm up to 9.50 mm. These orifice sizes correspond to type 1, type 2, and type 3 as classified by Zhou et al (2002) (with slight modifications) for horizontal pipe filling as shown in Table 4.2

Table 4. 2. Presenting ventilation classification

Ventilation Diameter (mm)	d/D	Classification
3.59 (A_v = 0.005)	0.07	Type 1
5.08 (A_v = 0.010)	0.10	Type 2 (lower)

7.18 (A_v = 0.020)	0.14	Type 2 (upper)
9.50 (A_v = 0.035)	0.19	Type 3

Discharge area (A_o) – three water discharge orifices were used for this investigation, with diameters of 12.7 mm, 25.4 mm, and the full pipe-cross sectional diameter of 50 mm. These orifice sizes were selected to bridge between experimental conditions related to the formation of gravity currents (i.e. full pipe discharge) down to more common blow-off valves. In all cases, the discharge was all directed downward.

Slope – Four slopes were used in the investigation: horizontal, and with angles of 2.5°, 5°, and 10°, measured with the horizontal.

The experimental variables and experimental measurements were normalized to facilitate a comparison with other conditions. The parameters used for normalization are the pipe diameter *D*, the pipe length *L*, gravity acceleration *g*, and these variables are presented in Table 4.3

Table 4. 3. Summary of normalization or variables and range considered in the research

Variables	Normalized variable	Normalized range of tested values
Slope – Slope	-	0.0, 0.025, 0.05, 0.10
Discharge area – A_o	$A_o^* = A_o/0.25\pi D^2$	0.0625, 0.25, 1.0
Ventilation area – A_v	$A_v^* = A_v/0.25\pi D^2$	0.0, 0.005, 0.01, 0.02, 0.035
Air pressure head - H	$H^* = (H_{air} - H_{atm})/D$	

Time – T	$T^* = T/(L/\sqrt{gD})$
Emptying flow rate - Q	$Q^* = Q/\sqrt{gD^5}$

4.2 Numerical investigation

A numerical model was developed to predict both the flow rate during the emptying process and the air pressure upstream of the pipe. The Runge-Kutta 4th order scheme was used to develop the solution to this problem. The water column was treated using the rigid theory method while the air pocket was modeled using the polytropic model.

4.2.1 Presentation of the numerical model

The numerical model used a system of algebraic and ordinary differential equations to represent key processes associated with the water discharge and related air pressurization changes. These equations have been selected from previous investigations, including the works by Zhou et al. (2002) and Fuertes-Miquel et al. (2019). These equations include the water phase continuity equation to relate volume changes to the pressure head at the discharge port and the ideal gas law to relate changes in the air volume, air inflow, and air pressure. Additional equations include the orifice equation to describe water outflow and energy losses. Figure 4.4 shows the schematic diagram of the key variables used to develop the numerical model.

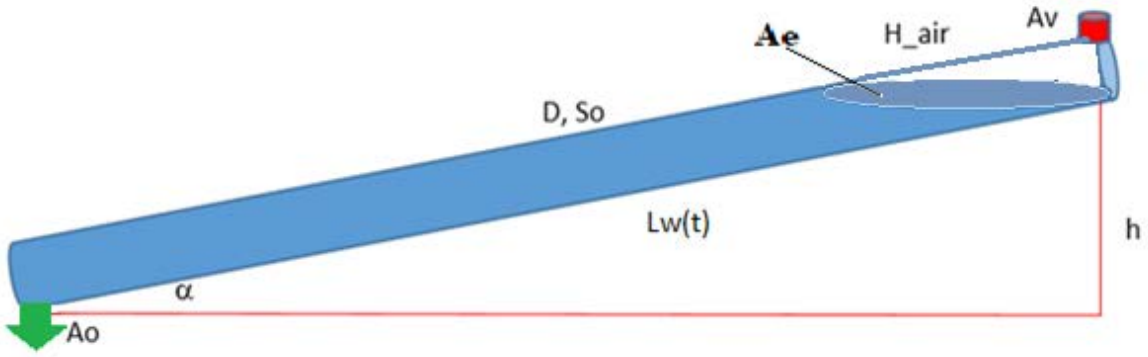

Figure 4. 4. Sketch of the model and key variables used for model development

$$A_e = \frac{\pi}{4} D \cdot \frac{D}{\sin \alpha}$$ Equation4. 1

$$A_e \frac{d}{dt}(h) = Q_{out} = C_d A_o \sqrt{2g(h - H_{air})}$$ Equation 4.2

$$H_{air} = H_{air\_abs} - H_b$$ Equation 4.3

$$Q_{air} = C_d A_v Y \sqrt{2g(H_{abs} - H_{air\_abs})}$$ Equation 4.4

$$Y = \left[\frac{k}{k-1} \left(\frac{H_{air\_abs}}{H_{abs}} \right)^{2/k} \frac{1 - \left(H_{air\_abs}/H_{abs} \right)^{(k-1)/k}}{1 - H_{air\_abs}/H_{abs}} \right]^{1/2}$$ Equation 4.5

$$\frac{dH_{abs}}{dt} = -k\frac{H_{abs}}{V_{air}}\left\{C_d A_o\sqrt{2g\left[h-\left(H_{abs}-H_{air\_abs}\right)\right]}-\right.$$

$$\left.C_d A_v Y\sqrt{2g\frac{\rho_w}{\rho_a}\left(H_{abs}-H_{air\_abs}\right)}\right\}$$

Equation 4.6

Where A_e is the area of ellipse, which is the assumed shape of the draining interface. H_{air} is the air pressure, H_{abs} is the absolute air pressure head, H_{air_abs} is the initial air pocket absolute pressure. *Y* is the expansion factor. K is the polytropic exponent and it was assumed to equal to 1.2. ρ_w and ρ_a are water and air density. H_{atm} is the atmospheric pressure head. Cd is the co-efficient of discharge assumed 0.65. It must be noted that the losses and viscous effects is this system of equations is taken of in the co-efficient of discharge. For fluids of different properties to water, the Cd assumption would be changed to suit those fluid properties or orifice opening.

The sequence of calculations used in the numerical model follows the flowchart is presented in Figure 4.5

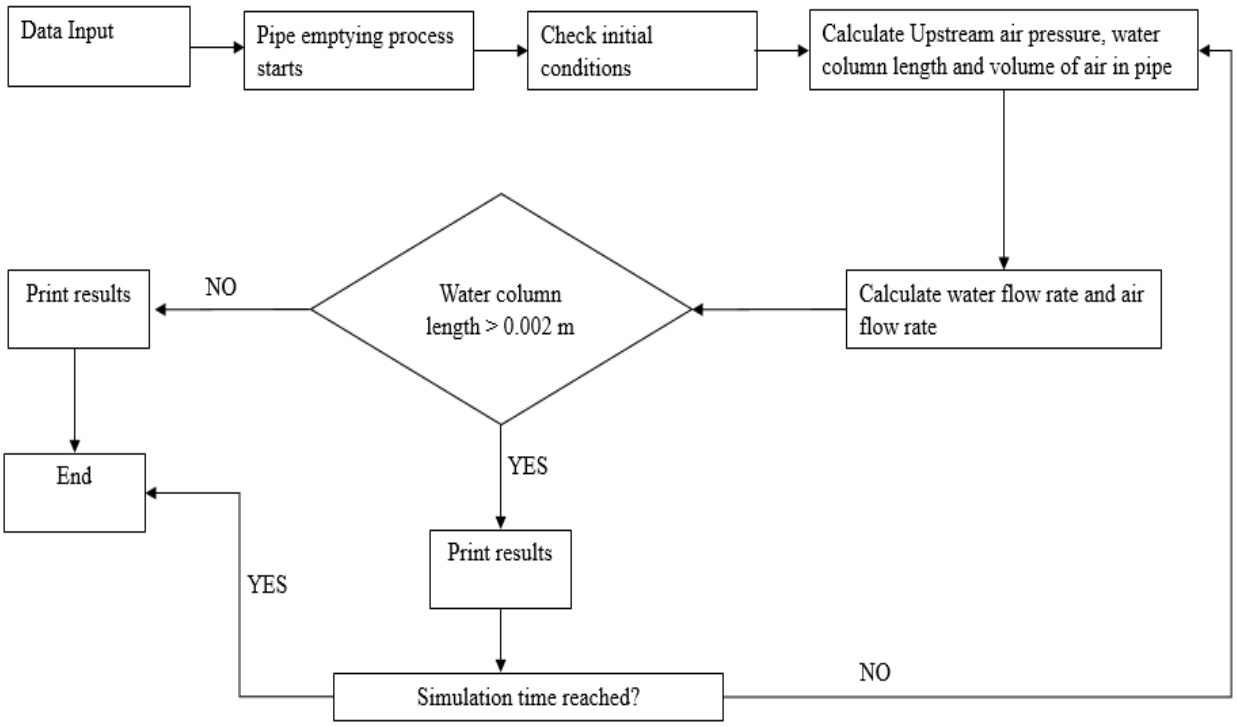

Figure 4. 5. Numerical model flow chart indicating all steps in the calculation.

4.2.2 Initial conditions, boundary conditions, and parameters

The model was developed assuming predetermined values for slopes, A_v, A_o, and pipe roughness throughout the emptying process. Initially, there is a zero flow rate in the system, and a small air volume is assumed to exist at the upstream end of the system prior to the simulation start. It was further assumed that the initial air pressure head prior to the discharge was equal to -0.001m, and the water outflow orifice discharge had a discharge coefficient of 0.65. Over time, conditions at the upstream and downstream end of the system are regulated by the air inflow described by

equation 4.4 and the water outflow described in equation 4.2, respectively. The simulation is completed when the length of the water column becomes smaller than 0.002m.

In particular, two groups of conditions were not represented in the model. First, full discharge conditions were not represented in the model. Such conditions resulted in the development of gravity currents with zero or smaller ventilations. The advance of these curved free surface interfaces into the water cannot be represented by the set of equations presented since it represents non-hydrostatic flow conditions. The second group of conditions not represented by the model was emptying involving zero ventilation. For these conditions, an alternative formulation for the air phase pressure, presented in equation 4.7 below would be required:

$$\frac{dH^*_{air}}{dt} = -k\frac{H^*_{air}}{V_{air}}\left\{C_d A_o \sqrt{2g[h-(H^*_{air}-H_{atm})]}\right\} \qquad \text{Equation 4.7}$$

However, it was considered that zero ventilation situations were not practically found in real water pipelines, and it was then decided not to include these in this work.

4.2.3 Numerical model implementation

The model was implemented using Microsoft Excel using Visual Basic for Applications (VBA) for its simplicity of implementation and to facilitate comparison with the experimental data that was already in MS Excel files. This tool is designed as a quick guide for expected air pressures and flow rates. The numerical scheme selected to solve the ordinary differential equations

(Equations 4.2 and 4.6) was the Runge-Kutta 4^{th} order scheme (RK4), as presented in (Press et al. 1989). This scheme was chosen because it has better accuracy than, for example, a simpler Forward Euler method to solve a system of ordinary differential equations. The Runge-Kutta used four trial steps and uses the weighted average to progress to the next time step, with the 1^{st} step being a Forward Euler scheme method to calculate the value for the initial estimates of the variable change over a time step.

Chapter 5

Results and analysis

This chapter presents the experimental and numerical results, and it is structured in the following sections:

- Section 5.1 presents the air-water interfaces observed for all experimental conditions along with a detailed explanation of flow characteristics.
- Section 5.2 presents a comparison of the experimental measurements of water outflows and air phase pressures along with the numerical model predictions for all cases with non-zero slopes, $A_v^*>0$, and $A_o^*<1$.
- Section 5.3 presents a comparison of the outflow rates for conditions that are analogous to a gravity current outflow ($A_o^*=1$) for varying slopes and A_v^* values with Benjamin (1968), Alves et al (1993) or alternatively a traditional orifice outflow condition when $A_o^*<1$.

- Finally, Section 5.4 presents air pressure results for zero-ventilation, large slope cases when (A_o^*=1) aiming to illustrate the negative effect of large discharges and poor ventilation to the internal pressures.

5.1. General description of air-water interfaces

Experimental observations have demonstrated a wide range of flow features and air-water interfaces during the emptying processes. Table 5.1 is a the summary of the different interfaces and the conditions required for each interface. They were five distinct types of air-water interfaces observed:

a) Gravity current -GCI – 4 out of 60 cases (6.5% of cases)

b) Dual gravity current – DGCI – 12 out of 60 cases (20% of cases)

c) Gulping – GULP – 8 out of 60 cases (13.5% of cases)

d) Gravity current and near-horizontal interface – NC-NH – 3 out of 60 cases (5% of cases)

e) Near horizontal interface – NHI – 33 out of 60 cases (55% of cases)

Table 5. 1 The different air-water interfaces and conditions in which they are formed

Ao*=Ao/Ap	**Slope**	**Ventilation - Av*=Av/Ap**				
		0	0.005	0.01	0.02	0.035
0.0625	0	GULP	GCI	GCI	GCI	GCI
	0.025	GULP	NHI	NHI	NHI	NHI
	0.05	GULP	NHI	NHI	NHI	NHI

	0.1	GULP	NHI	NHI	NHI	NHI
0.250	0	GULP	GCI	GCI	GCI	GCI
	0.025	GULP	NHI	NHI	NHI	NHI
	0.05	GULP	NHI	NHI	NHI	NHI
	0.1	GULP	NHI	NHI	NHI	NHI
1.000	0	GCI	DGCI	DGCI	DGCI	DGCI
	0.025	GCI	GC-NH	NHI	NHI	NHI
	0.05	GCI	GC-NH	NHI	NHI	NHI
	0.1	GCI	GC-NH	NHI	NHI	NHI

Figure 5.1 Schematic of the different interfaces as observed in the laboratory. A description and characterization of each interface is as follows:

- Gravity current: The gravity current was observed in cases where the was no ventilation on the upstream and the discharge orifice was the diameter size on the pipe (A_o^*=1). The discharge orientation did not affect the flow. Whether pointed downwards or oriented with the pipe a gravity current was formed. Systematic tests were performed only for the case with discharge oriented with the pipe. The air phase gravity current occupied roughly half the pipe diameter for horizontal slope; as sloped increase, the water depth at the discharge point decreased, however, the leading edge of the gravity current still occupied approximately 50% of the diameter. The thickness of air phase intrusion was not measured.

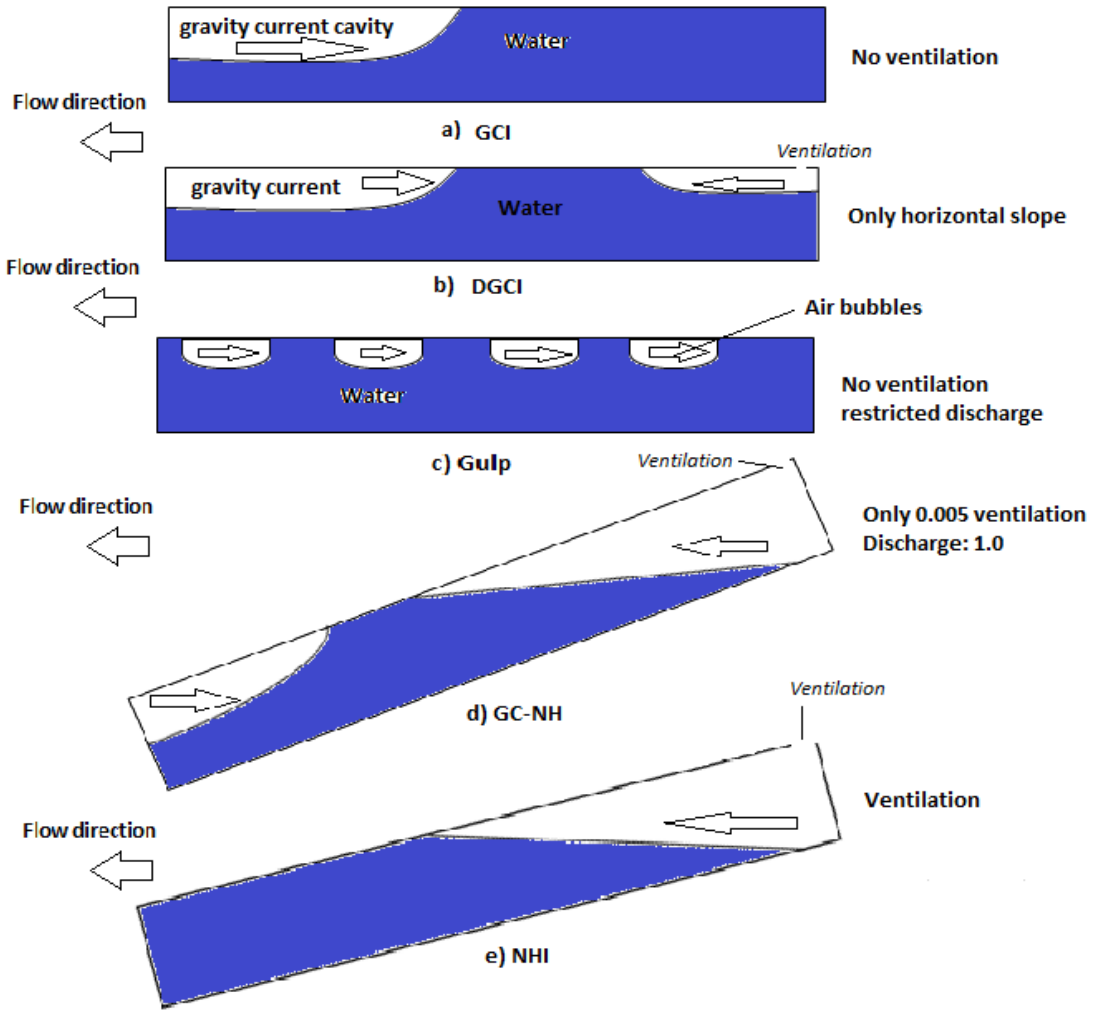

Figure 5.1 a) Sketch of the different air-water interfaces observed in the experimental runs

GCI

DGCI

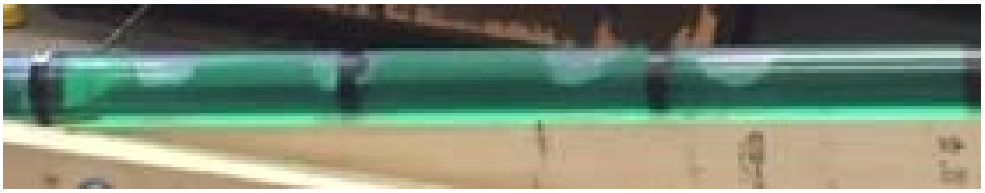

GULP

GC-NH

NHI

Figure 5. 1 b) picture of the different air-water interfaces observed in the experimental runs.

- Dual gravity current (DGCI): The Dual gravity current was formed only in horizontal slopes with $A_v^* > 0$. The second, smaller air intrusion was initiated as soon as the downstream gate was opened, and is explained by the sub-atmospheric conditions at the

full-pipe flow side of gravity currents, as explained by Benjamin (1968). The gravity current from the pipe discharge point was always much thicker (~50% pipe) than the one formed at the ventilation point, and as so it moved faster. The two GC fronts eventually met and flow then the system continued the emptying in free surface flow mode.

- Gulping: This condition was observed for $A_v^*=0$ and $A_o^*<1$. According to Geiger (2012) the limit for this kind of interface is discharged orifice equal to half the pipe diameter and smaller. Gulping happens when the is a counter-current outflow of water and intake of air, resulting from sub-atmospheric conditions created inside the pipe as water flows out. The air moves in the form of bubbles on top of the pipe from the downstream discharge port to the non-ventilated upstream end.
- Gravity current with near-horizontal interface (GC-NH): This condition was only observed in cases where a non-zero slope, $A_o^*=1$ and $A_v^* = 0.005$. In these conditions, a gravity current is formed on the downstream side and moved upstream. The near horizontal surface is formed at the upstream end due to the ventilation advanced gradually downstream. Given that the volumetric air inflow at the upstream end is small, this enabled the presence of the GC at the downstream end, unlike the NHI cases. When the two interfaces met, free-surface flows existed throughout the pipe.
- Near horizontal interface (NHI): This was the most commonly observed air-water interface, and was formed in cases of positive slopes and non-zero ventilation for restricted discharge orifice sizes, $A_o^* <1$. This air-water interface was also observed when $A_o^* =1$ and $A_v^* > 0.005$. The near horizontal interface only formed at the upstream side of the pipe and

moved towards the downstream. The interface elongates as more water is drained from the pipe. The elongation extends with slope steepness. The steeper the slope, the longer the elongation and the milder the slope, the less elongated is the interface. This interface is formed when enough air is introduced into the pipe to cause a flow rate fast enough not to allow any air to enter from the downstream side.

5.2. Air pressure measurements

Figure 5.2 shows the graphs of air pressure changes versus time for 2.5 degree slope, $A_o^* = 0.0625$ discharge outlet and arranged from right to left the different ventilation from $A_v^* = 0.005$, 0.010, 0.020, 0.035. Air pressure head results were normalized as $\left(\frac{H^*-H_{atm}}{D}\right)$ and time was normalized as $\left(\frac{T}{L/\sqrt{gD}}\right)$. These results were consistent for all cases, with smaller A_v^* resulting in stronger negative air pressures and smaller A_o^* resulted in weaker negative air pressures.

Conditions involving $A_v^* = 0.005$ were among the ones leading to the largest sub-atmospheric pressure. This is because the small ventilation prevents an adequate air inflow into the pipe to fill balance the outflow of water draining out. Unlike this case, conditions with $A_v^* = 0.020$ and 0.035 presented very small air pressure changes while the $A_v^* = 0.01$ ventilation had an intermediate effect on the sub-atmospheric pressures. Typically, the sudden opening of the discharge orifice caused a spike in negative pressure at the upstream side as the liquid starts to move and the pressure

increases back to atmospheric pressure as more air is admitted into the pipe through the ventilation orifice as water drains out of the discharge orifice.

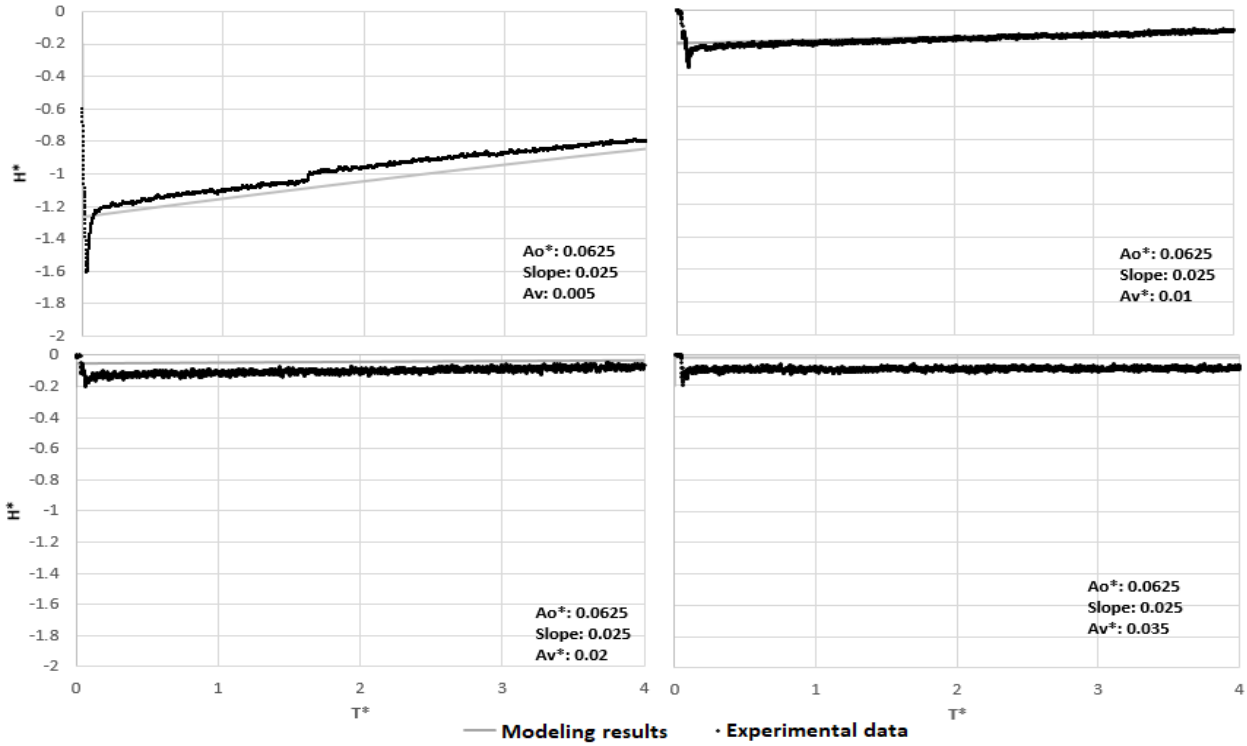

Figure 5. 2 Air pressure rate for Ao*=0.0625 discharge orifice and different ventilation: slope 0.025

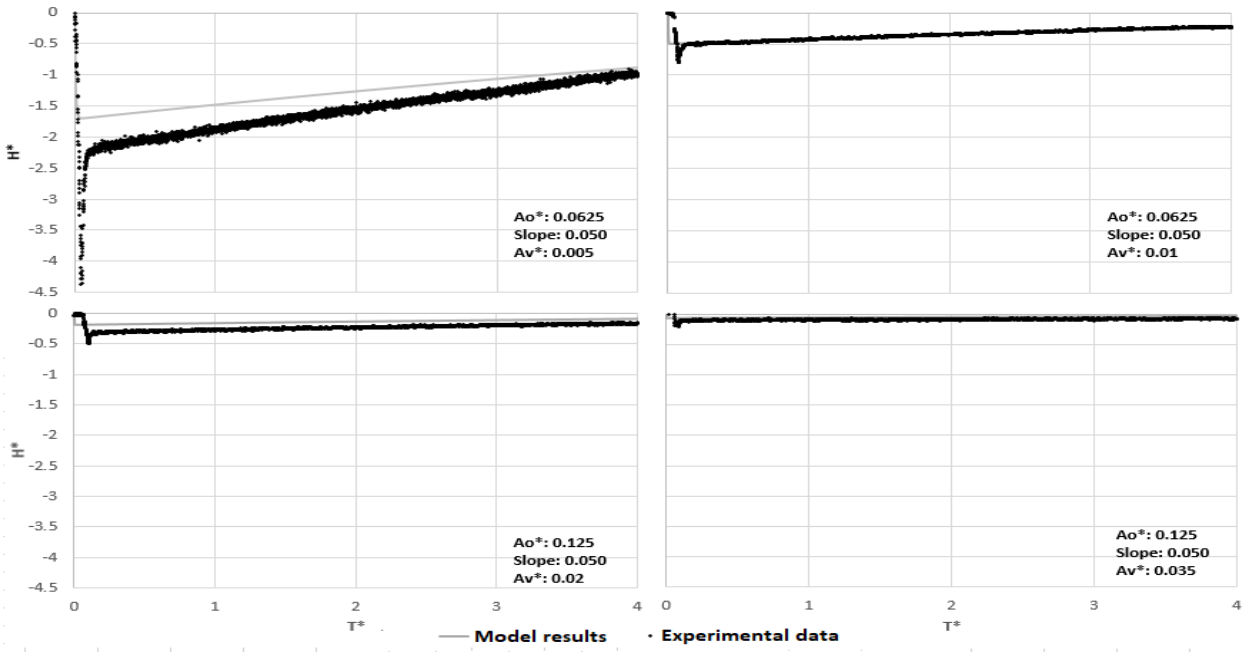

Figure 5. 3. Air pressure rate for Ao*=0.0625 discharge orifice and different ventilation: slope 0.05

Results involving the 2.5 degree slopes also presented smaller air pressure changes when compared with the other non-zero slopes. As is shown in Figures 5.3 and 5.4, steeper slopes resulted in more negative air pressures. This is an expected result, because of the larger elevation difference between the endpoints of the water column with steeper slopes, with the downstream end at atmospheric pressure.

Figure 5.5 presents the results of the air pressure at the upstream side of the pipe for $A_o^* = 0.25$ discharge orifice. The change in discharge orifice size resulted in a similar relationship between ventilation size and air pressure as in Figures 5.2 to Figure 5.4. The change in discharge orifice

size resulted in no negative pressure spikes at the initial stages of flow. This is because the larger discharge orifice mitigates the development of transient type pressure waves through the pipe.

The air pressure experimental data was compared with the modeling results for the restricted discharge, ventilated cases, and positive slope cases. The comparison results are also presented in Figure 5.2 to Figure 5.7 for the $A_o^* = 0.0625$ cases. As can be noted from these figures, the numerical model predicted air pressure fairly accurately for smaller ventilation conditions ($A_v^* = 0.005$ and 0.01). Conversely, for larger ventilation ($A_v^* = 0.02$ and 0.035), the model underpredicted the results. This would be caused by the rapid change in the ellipse shape when the ventilation is larger while the model maintains the same shape throughout the emptying process.

A different outcome was observed for the $A_o^* = 0.25$ discharge port. In this case, conditions involving larger ventilations namely $A_v^* = 0.02$ and $A_v^* = 0.035$ had in general more accurate results than the smaller ventilations with $A_v^* = 0.01$ having the most inconsistent results. The results for $A_v^* = 0.005$ improved with slope steepness. Possible reasons for the error in the experimental data and modeling results would be that the water discharge rate for the $A_o^* = 0.25$ discharge port, offers a balance for water column leading to the shape of the ellipses remaining relatively constant throughout. This was not observed on the smaller ventilations where the interface from the upstream side remained almost perpendicular to the pipe walls for about 2m of the pipe length.

The model can be improved to represent the initial negative pressure spikes in the A_o^* = 0.0625 discharge and also for the simultaneous water discharge and air uptake at the discharge opening for the A_o^* = 0.25 discharge port.

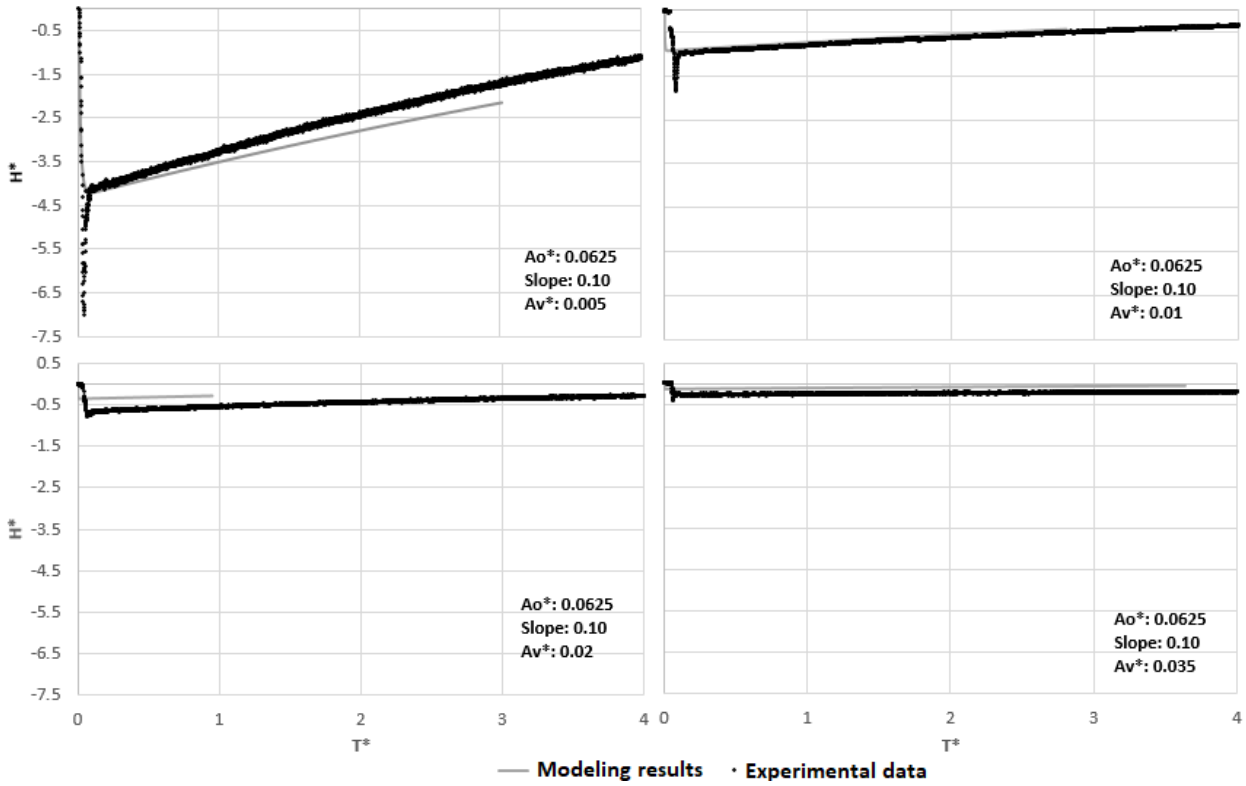

Figure 5. 4 Air pressure rate for A_o^*=0.0625 discharge orifice and different ventilation: slope 0.10

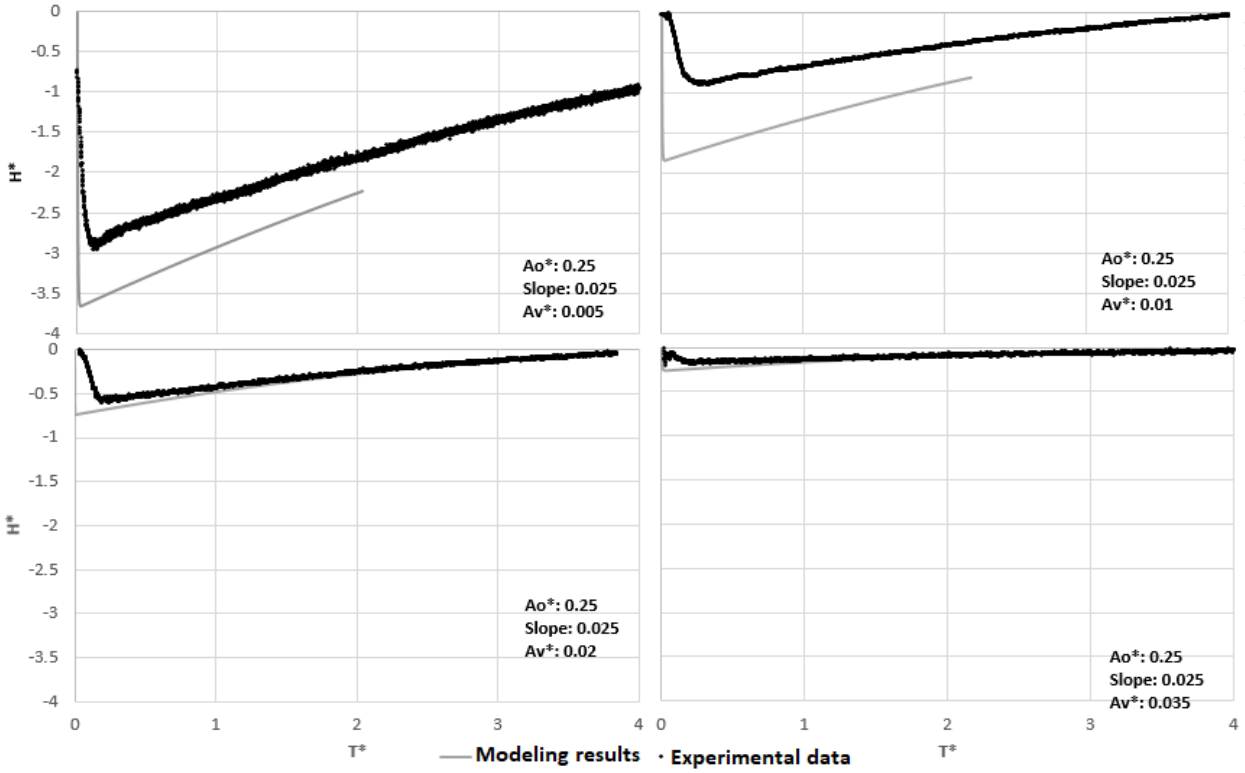

Figure 5. 5 Air pressure rate for A_o^*=0.25 discharge orifice and different ventilation: slope 0.025

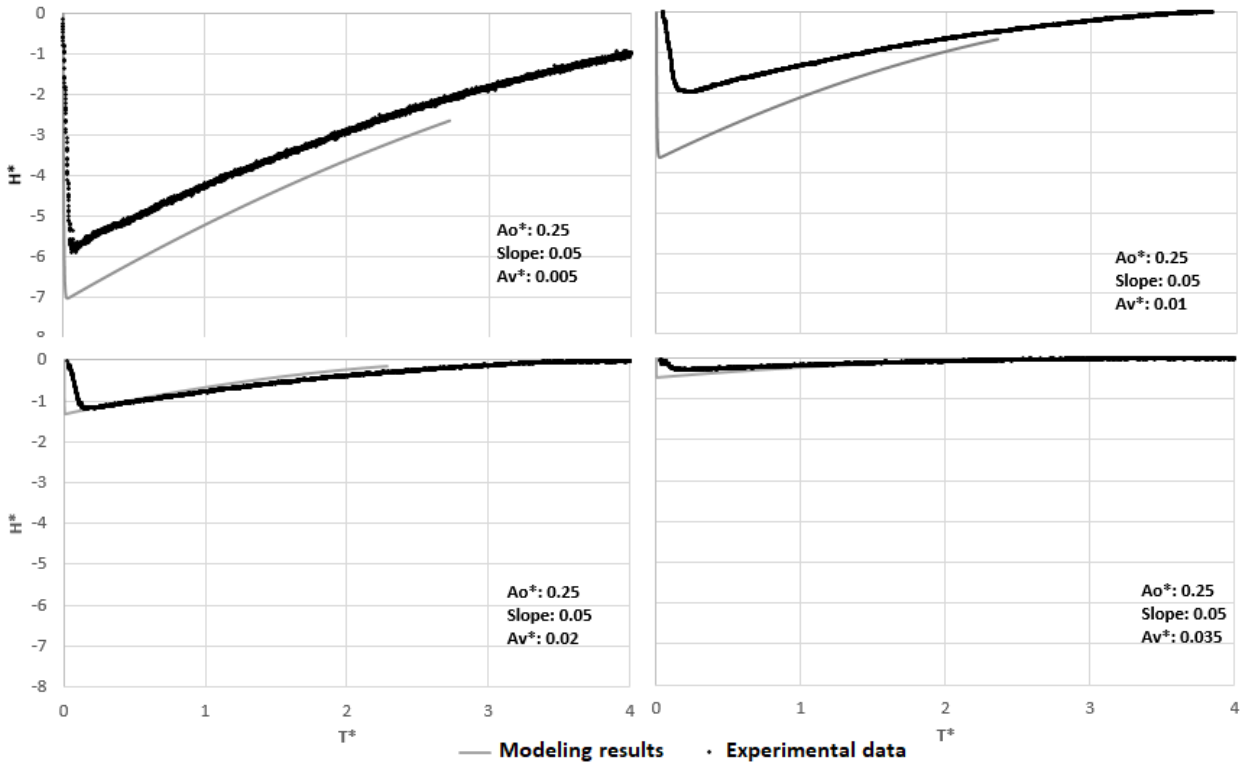

Figure 5. 6 Air pressure rate for A_o^*=0.25 discharge orifice and different ventilation: slope 0.05

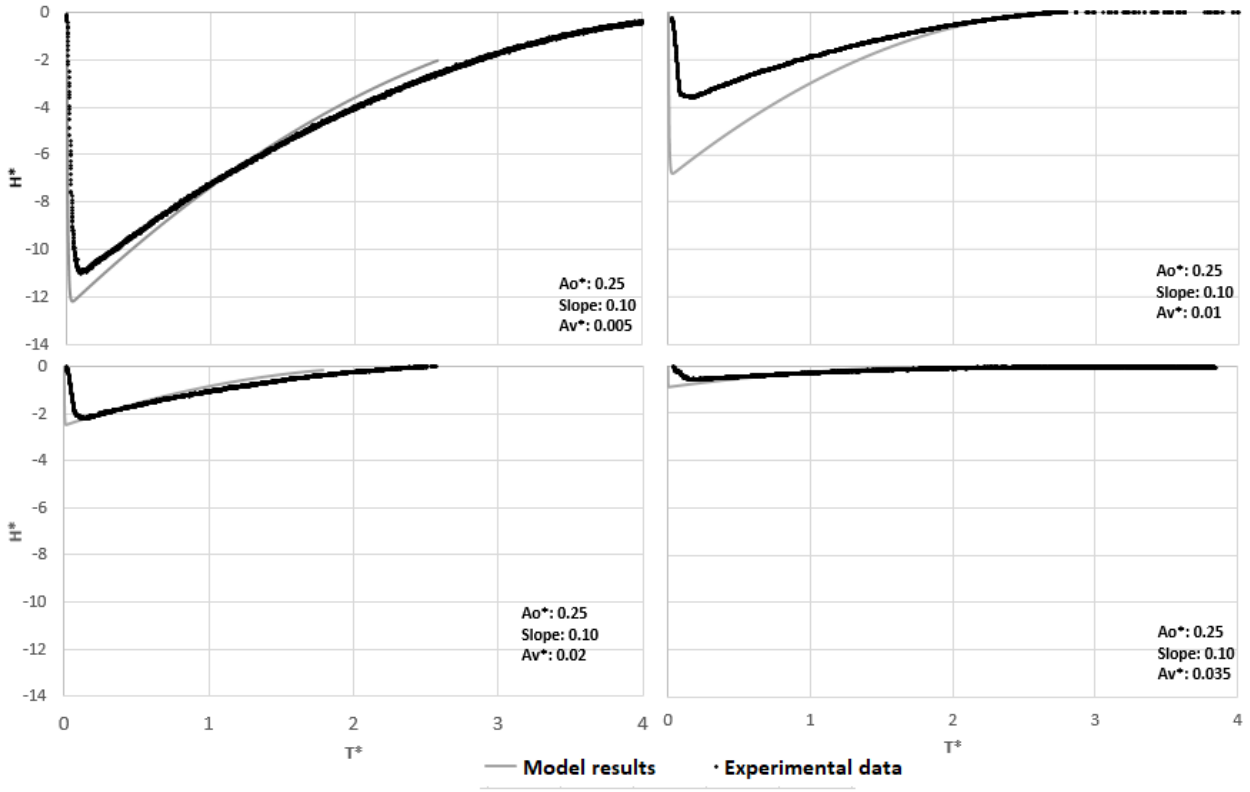

Figure 5. 7 Air pressure rate for A_o^* = 0.25 discharge orifice and different ventilation: slope 10 slopes

5.3. Water outflow measurements

Figure 5.8 presents the outflow results for the different ventilation for conditions using 2.5 degree slope and ventilation A_o^* = 0.0625. As can be noted, flow rate (normalized by $\sqrt{gD^5}$) increased with the ventilation up to A_v^* = 0.02. This is explained that larger orifices decreased the internal negative air pressures, facilitating the water outflow. However, this increase in flow rate was not significant across ventilation sizes. This was probably because the discharge rate was more limited

by the discharge orifice dimensions rather than the ventilation. The 14% increase in ventilation represented an approximately 10% increase in flow rate.

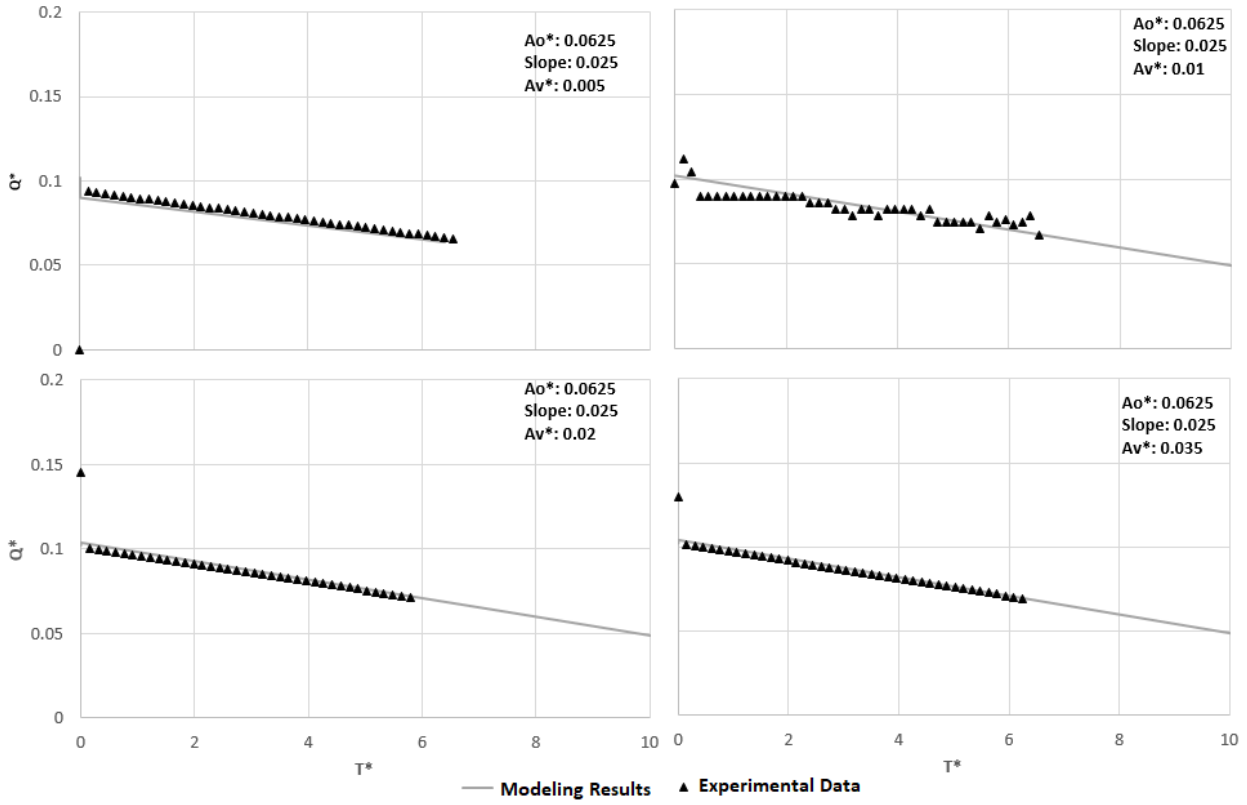

Figure 5. 8 Outflow rate for A_o^*=0.0625 discharge orifice and different ventilation: slope 0.025

The increase in slope gradient also showed to increase the flow rate. This was true for the different slopes as shown in Figure 5.9 and 5.10. The slope had a greater influence on the outflow rate than the ventilation. This was an expected result because the outflow rate depends on the potential

energy of the water within the pipe, and larger slopes provide this greater pressure head and larger flow rate. The increased slope gradient resulted in an approximately 50% increase in flow rate.

Figure 5.10 shows the flow results for the A_o^* = 0.25 discharge port. From these results, it can be noted that increased ventilation resulted in an increased discharge rate. The percentage increase in discharge due to ventilation was much bigger than for A_o^* = 0.0625. The was an approximately 50% increase in flow rate as a result of a 14% increase in ventilation. The slope had a greater effect on the flow rate than the ventilation as it resulted in an approximately 75% increase in the flow rate.

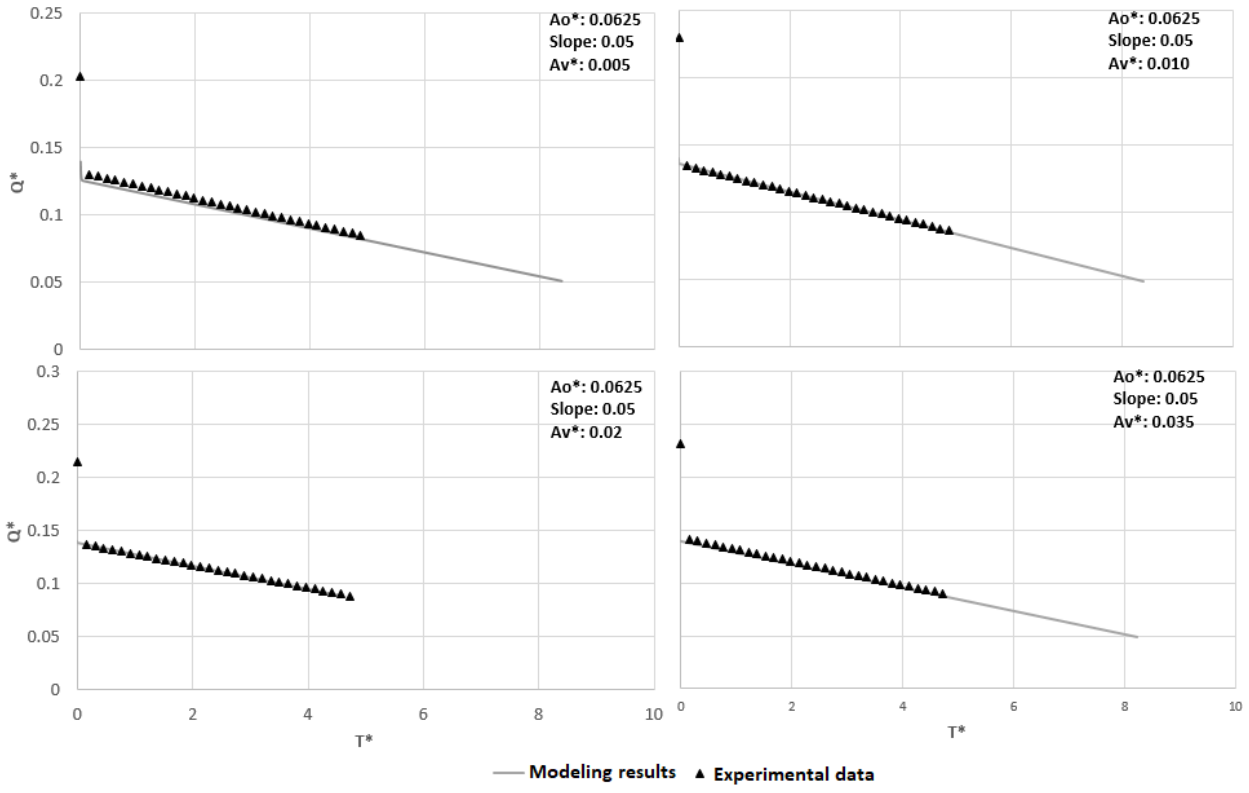

Figure 5. 9 Outflow rate for A_o^*=0.0625 discharge orifice and varying ventilation, with slope 0.050

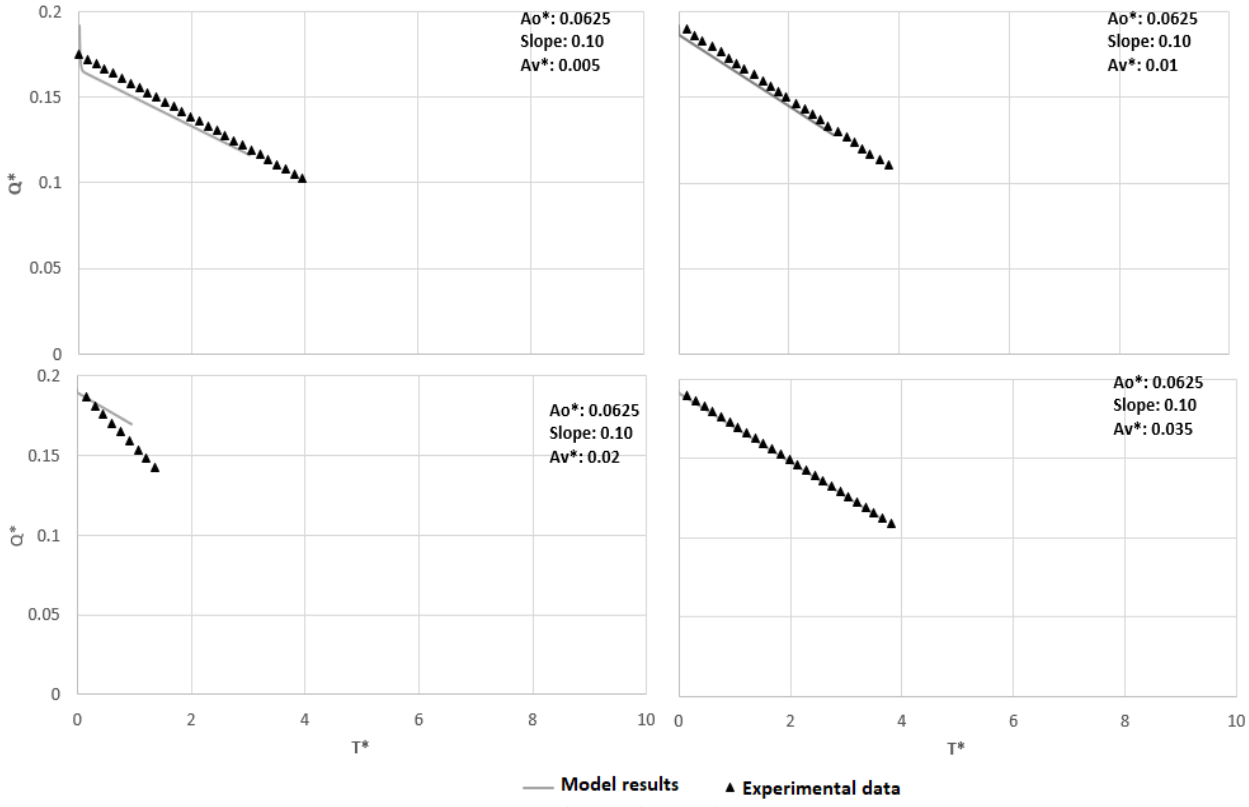

Figure 5. 10 Outflow rate for A_o^*=0.0625 discharge orifice and different ventilation: slope 0.10

Figure 5.11 to 5.13 continue to present a comparison of the experimental measurements of the outflow rate data and modeling flow rate predictions, with a generally good agreement. In the case of 0.10 slope, the were slight differences between the A_v^* = 0.005 result and the A_v^* = 0.02 result. In all instances, the model overestimated the flow rate. Looking at the typical picture (Figure 5.11) for 10 slopes slope and A_v^* = 0.035 it can be observed one example where the NH interface breakdown at the early stages of the emptying, potentially interfering with the modeling assumptions and helping in the discrepancy between the model and experimental results.

Figure 5. 11. Typical early stage air-water interface for 10 degree slope and $A_v^* = 0.035$, $A_o^* = 0.25$ prior to becoming near horizontal

Figure 5.12 and Figure 5.13 show the experimental data and modeling results comparison for the $A_o^* = 0.25$ discharge port. There was a good agreement between the experimental data and model results for the slower flow rates namely $A_v^* = 0.005$ and $A_v^* = 0.01$. For the faster flow rates there was a discrepancy between the model results and the experimental data caused by data collection errors. This was because the short pipe length and fast draining flows. This resulted in a compromised water collection process for calculation the flow rate.

The flow rate was found to decrease with time. This is because of the shorting of the water column resulting in decreased hydraulic head. Ventilation was found to have a bigger influence on the flow rate than for the $A_o^* = 0.0625$ cases. This is because the more air that can be introduced into the system, the more water that can be displaced out of the system. The introduction of atmospheric

pressured air greatly reduces the negative pressures inside the pipe, leaving to weaker vacuum effect and therefore faster flow rate.

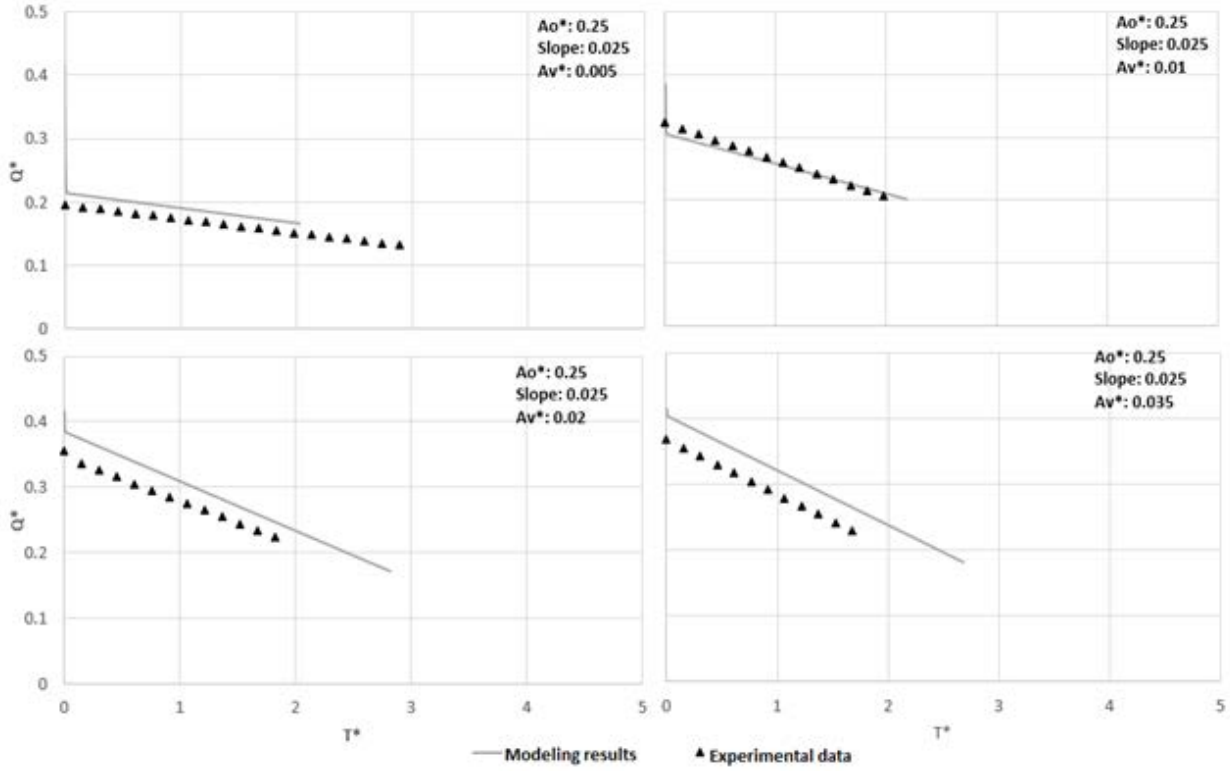

Figure 5. 12 Outflow rate for A_o^*=0.25 discharge orifice and different ventilation: slope 0.025

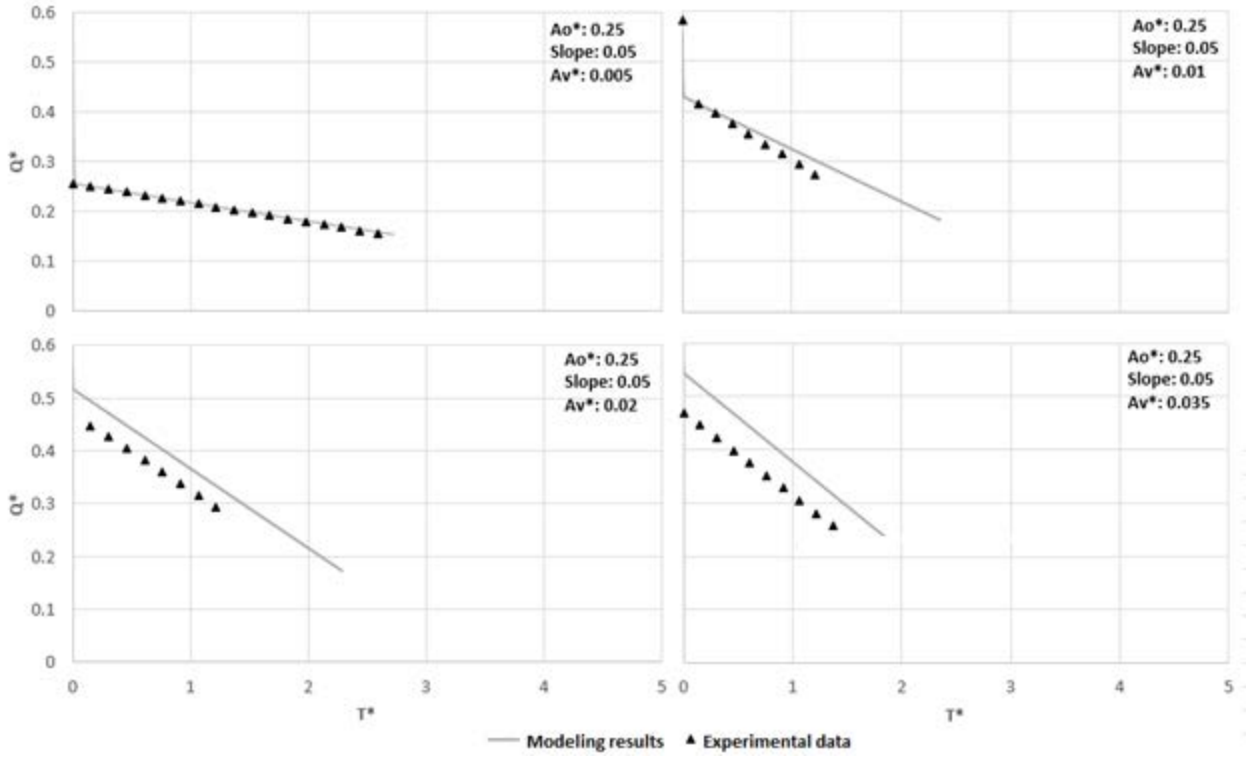

Figure 5. 13 Outflow rate for A_o^*=0.25 discharge orifice and different ventilation: slope 0.05

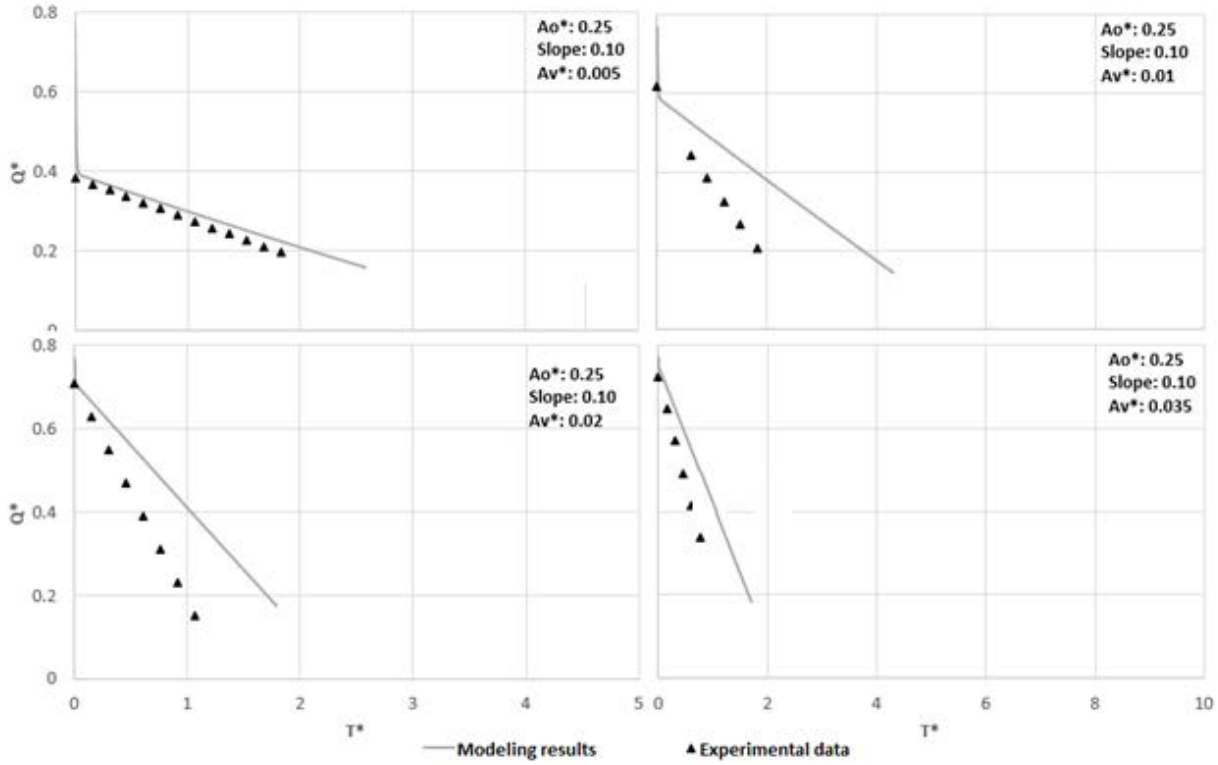

Figure 5. 14 Outflow rate for A_o^*=0.25 discharge orifice and different ventilation: slope 0.10

5.4. Comparison of outflow rates in horizontal conditions

Figure 5.15 shows the flow rates for the horizontal slope with different size discharge ports and ventilations sizes. From the figure for $A_o^* = 0.0625$ the no ventilation ($A_v^* = 0.0$) resulted in the slowest flow rate followed by $A_v^* = 0.005$. The flow rates for $A_v^* = 0.01$, 0.02 and 0.035 were approximately equal. This shows that for this condition, as the ventilation size increase, the discharge orifice size becomes the limiting factor for flow rates. In the case of $A_o^* = 0.25$, the ventilation size does determine the discharge flow rate. Interestingly zero ventilation case had a

positive gradient, meaning the flow rate increased as the water drained out of the pipe. This is because with the smaller ventilation and with the absence of extra potential energy due to the horizontal slope the rate of water outflow was not so large to the point to provoke strong negative air pressures, which would decrease the outflow rate.

For the remaining discharge orifice cases, it was clear that larger the ventilation size increased the outflow rate. Ventilation had a very significant effect in the rate of outflow decrease over time as $A_v^* = 0.0$ and $A_v^* = 0.005$ had smaller change in outflow rates over time when compared with $A_v^* = 0.01$, 0.02 and 0.035. For conditions involving $A_o^*=1.0$, The flow rates for the different ventilation sizes crossed at a common time, approximately $T^* = 1.3$. This is approximately the time when the two gravity currents of DGCI conditions merged and formed free surface in the pipe. Coincidentally at this point, all the flow rates are equivalent to the flow rate as predicted by the orifice equation at $Q^* = 0.19$ for discharge diameter equal to half pipe diameter.

The results with $A_o^*=1.0$ were compared with the Benjamin 1968 theoretical gravity current. The was good agreement between the theoretical and experimental data at the start of the flow. In reality, the flow rate decreases over time and therefore the theoretical gravity current celerity does not hold throughout the pipe emptying process.

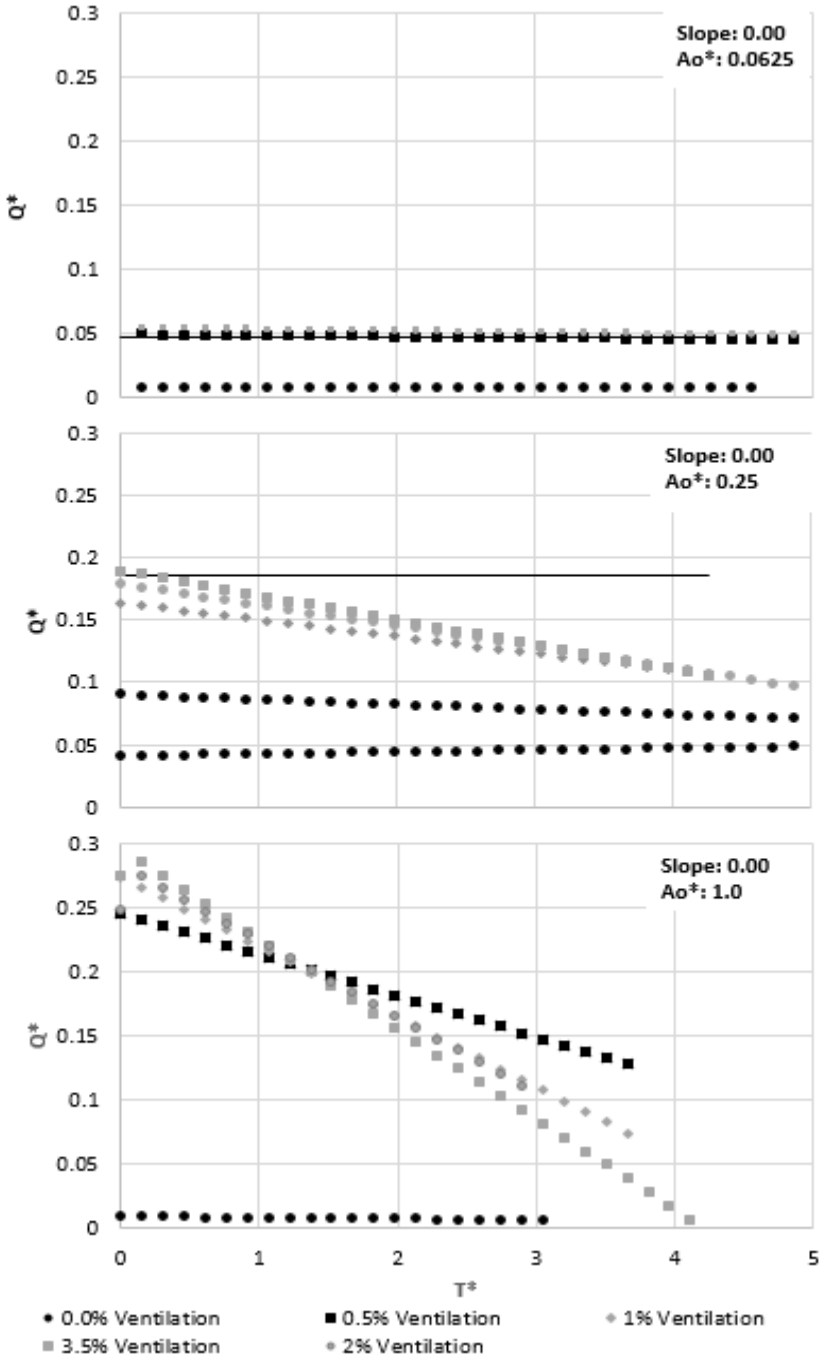

Figure 5. 15 Comparison of flow rate for horizontal slope and varying discharge orifice and ventilation

Figure 5.16 and Figure 5.17 Show the comparison of flow rate for varying slopes. From Figure 5.15, the flow rates were compared with the flow rate as predicted with the orifice equation and for all ventilated pipes and mild slope, 0.00 and 0.025, the orifice equation reasonably predicted the flow rate at the start of flow. Zero ventilation was not well predicted because this does not conform to the orifice equation because of the restriction in the flow rate resulting from the negative pressure caused by the initiation of flow. For steep slopes (0.05 and 0.1) the orifice equation worked well for only the start of flow. This is because as the water drains out, the is a large variation in head causing flow due to the steepness of the pipe. Interestingly the flow rate for the zero ventilation condition showed mixed results. The 0.025 slope condition had flow rate lower than the horizontal condition. This was caused by the discharge orifice position, such that the weight of the water for the 0.025 slope restricted the uptake of air thus slowing down the flow rate. The slope 0.1 condition had the slowest flow rate, due to the magnitude of the negative pressure created upstream.

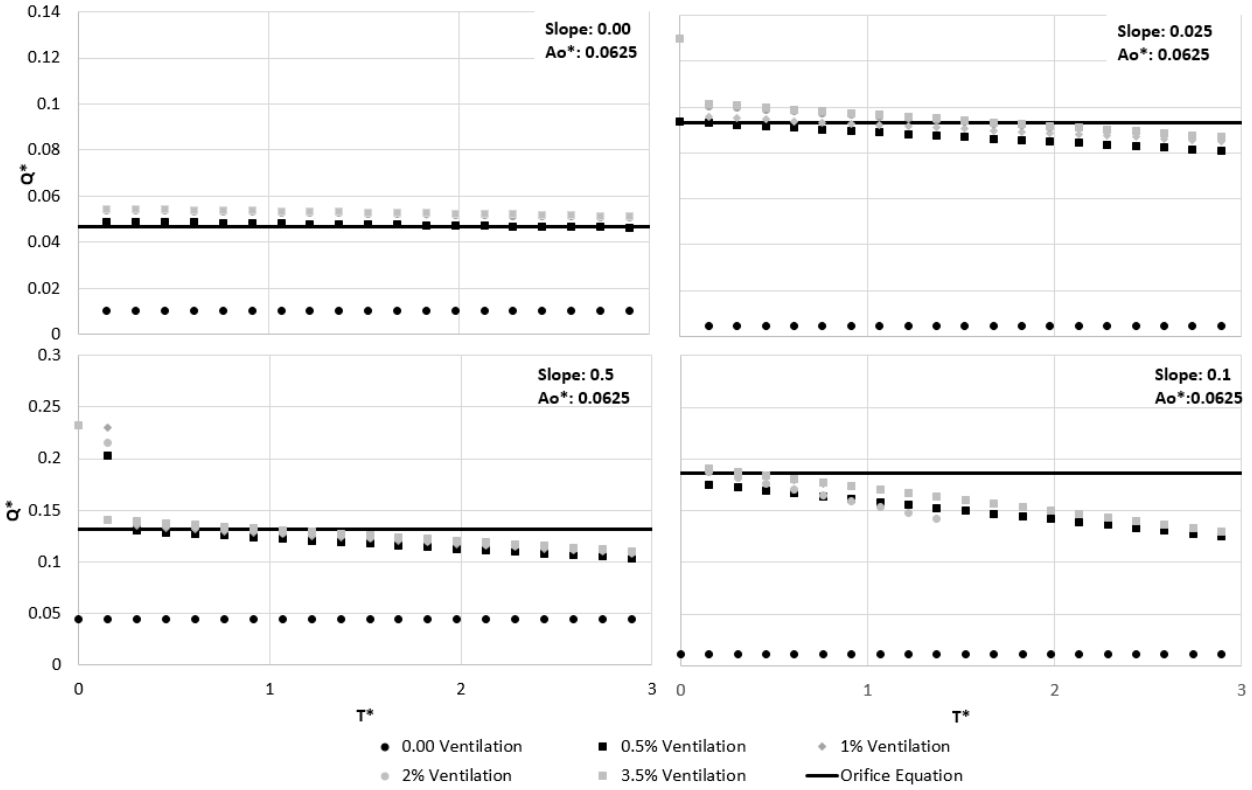

Figure 5. 16 Comparison of flow rate for varying slope and discharge orifice $A_o^* = 0.0625$

Figure 5.17 shows the flow rate as compared for varying slopes for the $A_o^* = 0.25$ discharge port. The gulping flow rate from this discharge port, $A_o^* = 0.25$ and mild slopes 0.000 and 0.025 were within an equal range. One plausible explanation for this is that for this size of port (diameter half that of pipe) and slopes, the is a simultaneous exchange of water and air which leads to restrictions to the amount of water that can be discharged and air that can be taken in to the pipe. The ratio of water to air is independent of the slope or pressure inside the pipe. The 0.05 and 0.1 slopes the slope magnitude has a direct impact on the flow rates. An approximately 100% slope increment resulted in approximately 50 % flow rate increment. Comparison with the orifice equation shows that it's accurate to predict the start flow rate for only the well ventilated cases, type 2 upper and

type 3. Type 1 and type 2 lower ventilations have a high magnitude of negative air pressure than restriction the flow rate.

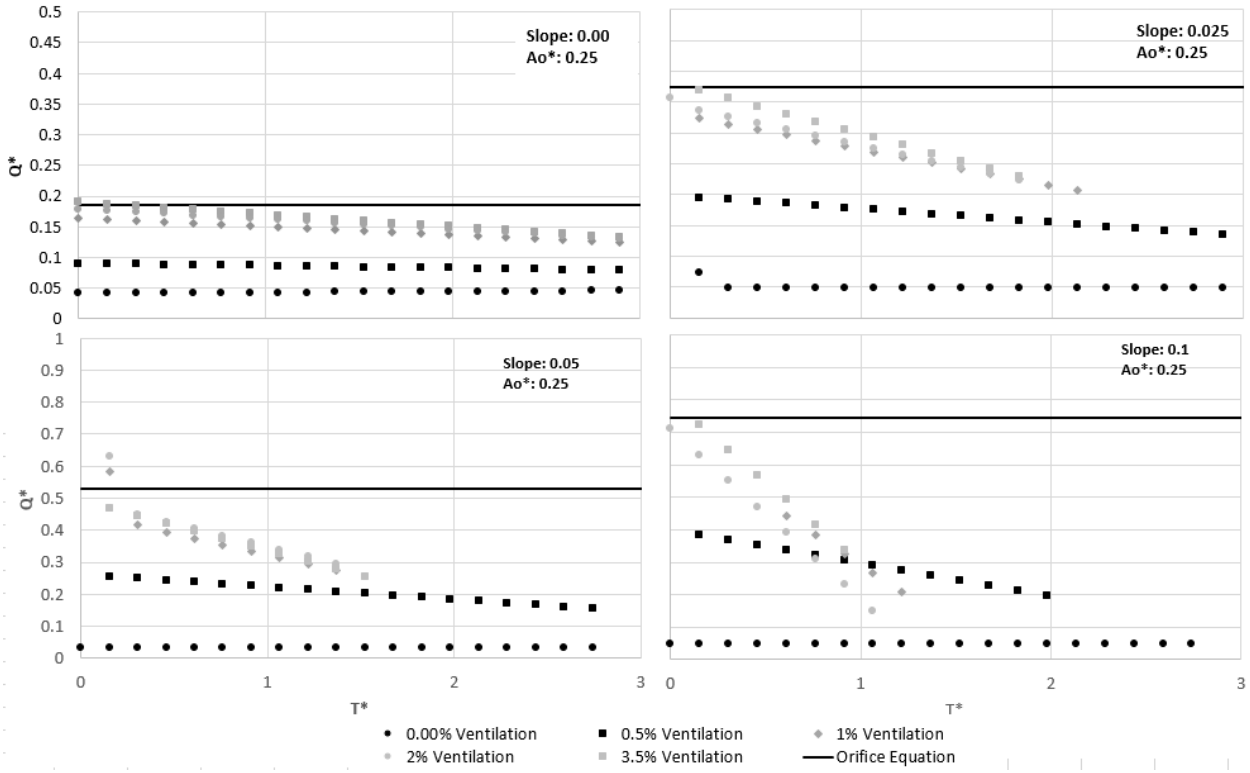

Figure 5. 17 Comparison for outflow rates for varying slope and ventilation conditions considering discharge orifice $A_o^* = 0.25$

5.4. Comparison of outflow rates for large discharge port (Ao*=1.0)

Figure 5.18 presents the discharge flowrate for $A_o^* = 1.0$ arranged by slope sizes. The discharge flow rates increased by slope and ventilation. Big ventilation sizes resulted in fast flowrates, while small ventilation sizes resulted in slower flow rates. The same was true for the slope. The steeper the slope the faster the flow rate. A comparison was made with theoretical data for the inclined pipe flow rates based on the interpolation of Alves et al. (1993) data. Interpolation was made for

the smaller slopes, 2.5 slopes and 5 slopes as the data is for 0, 10, 20 up to 90 slopes. It is worth noting that Zukoski (1966) observed that viscous and surface tension had a significant effect on the celerity of gravity currents and therefore a wide range of data exists for the same inclination slopes. The experimental data were in good agreement (within the scatter) with the theoretical data. Slope positively affects the celerity of the gravity current

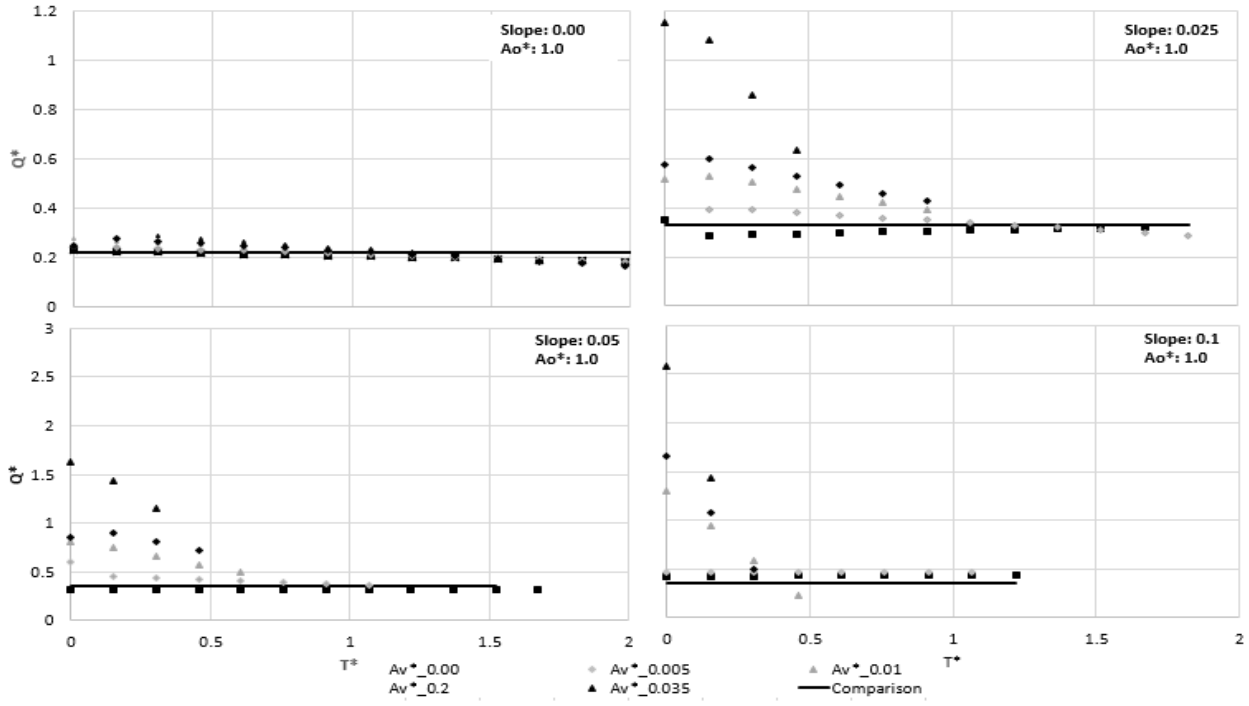

Figure 5. 18, Comparison of outflow rates for varying slopes and ventilations for A_o^*=1.0

5.5 Air pressure measurements for steepest slopes and small ventilation conditions

Figure 5.19 shows the comparison of the effects of 0.05 and 0.1 slopes and smallest ventilation (A_v^* = 0.0 and 0.005) on the air pressure during pipe emptying. It can be noted that for cases where

the is no ventilation ($A_v^* = 0.0$) the is oscillatory pressure at the initial stages of outflow, analogous to a spring mass system studies by Martin (1976), Zhou et al. (2002) and Vasconcelos and Leite (2012) for air-water flows with no ventilation.

The minimum air pressure is approximate twice as negative as the air pressure when A_v^*=0.005, highlighting the importance of operational conditions of ventilation valves. The oscillatory pressure is different in magnitude for the different slopes but lasts the same period given that it is based on small air pocket volumes that were residual in the apparatus prior to the valve opening. One important outcome of these measurements is to confirm that poorly ventilated pipelines undergoing large, uncontrolled emptying (for instance resulting from a major rupture) could experience low and damaging pressures.

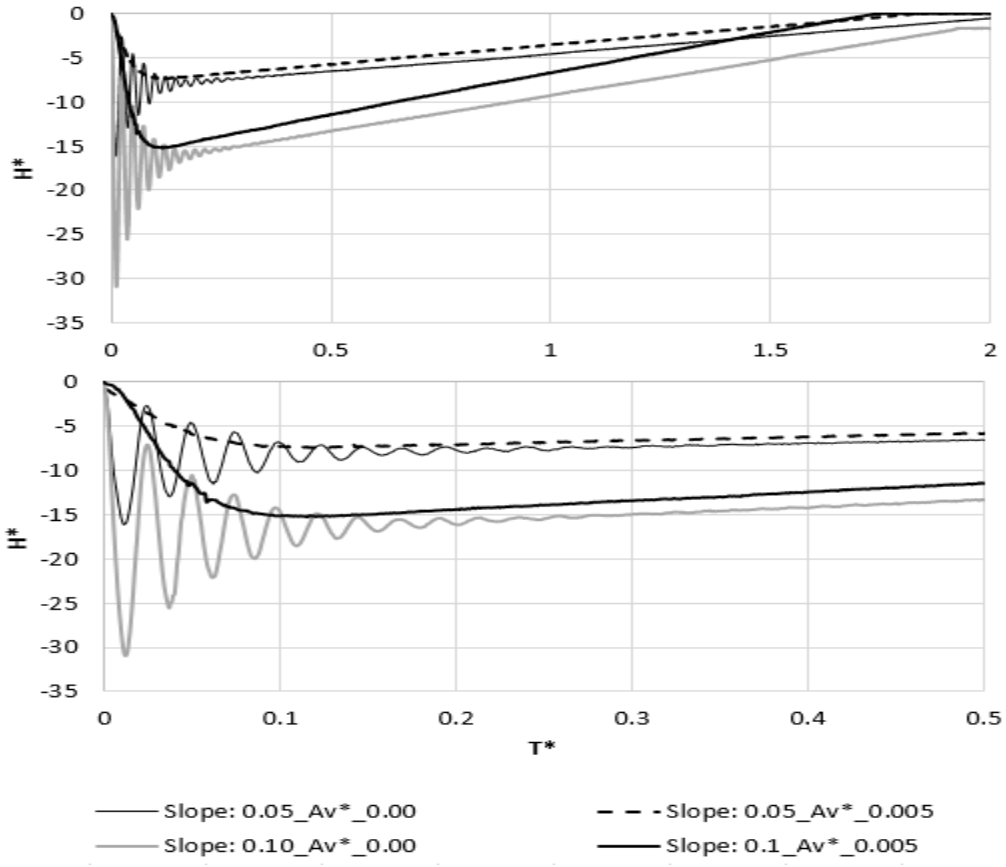

Figure 5. 19 Comparison of air pressure within the pipeline following large discharge ($A_o^* = 1$), steep slopes ($S_o = 0.05$ and 0.10) and small ventilation ($A_v^* < 0.005$)

6 Conclusion

This research set out to study two phase flows in pipe emptying. The objective was to describe the different air-water interfaces that are formed when a pipe empties with the hope of also defining what conditions lead to those interfaces. In this regard the focus of the research was to evaluate the main parameters that affect or influence the emptying process. These being slope of pipe, ventilation and discharge port. This research is also important to highlight how pressure variations and outflow rates are affected slope, ventilation and discharge orifice in pipe emptying. This was done through experimental work and easy to use numerical tool.

One of the questions that this work was intended to answer is the possibility of a secondary gravity current in horizontal pipes when upstream ventilation. It can be concluded that upstream ventilation in horizontal pipes does cause a secondary gravity current. This gravity current moves in the same direction as the flow and its size is determined by the diameter of the ventilation orifice. This gravity current has all the different flow zones as the primary gravity current.

The conditions for the gravity current to occur are different between sloped pipes and horizontal pipes. Even though a gravity current will occur in a ventilated horizontal pipe, the same is not true for sloped pipes. This is because for sloped pipes, the ventilation leads to high flow rates which prevents the formation of gravity current.

The flow rate variations over time were measured and it can be concluded that the flow rates decrease with time during the emptying process. It was also found that the sub-atmospheric pressure affects the flow rate negatively. This is because of the vacuum effect created by the strong negative pressures. Ventilation had limited effect on the flow rate for the $A_o^* = 0.0625$ cases, but had a bigger influence on the flow rate for $A_o^* = 0.25$ cases. This shows that the discharge orifice can be a limiting factor to flow rates.

The experimental work also studied the changes in the upstream pressure during pipe emptying conditions. The changes in potential energy in the pipe created by varying slopes was found to be a dominant parameter in pressure changes upstream for small ventilation conditions. Large ventilation ($A_v^* >= 0.02$) have maintained air pressurization change to a minimum. The was a clear inverse correlation between the negative pressures and flow rates, with slope and ventilation controlling the flow rates. Experiments indicated, as expected, that large slope and large ventilation resulted in a very fast flow rate. The practical observation is that exposed pipelines that are damaged and rupture could have a very large rate of emptying depending on its slope and available ventilation. However, limited ventilation has created an air pressure vacuum that has decreased outflow rates. These vacuum levels, however, could be in some cases too large and lead to damaging negative pressures in water pipelines.

The experimental work developed in this research indicated that the are five distinct types of air-water interfaces in water pipelines during emptying processes. These depend on the different combinations of ventilation, slope, and discharge orifice size, with the near horizontal interface

being the dominant type when the is ventilation. In conditions where no ventilation existed, two types of air-water interfaces could occur, namely gulping and gravity current. When the discharge orifice is the same size as the pipe, a gravity current was observed to occur regardless of slope and ventilation size. This clearly shows that when the air-water interface is mostly influenced by the geometry of the opening and not by the ventilation when discharge area was equal to the pipe area. For smaller discharge areas, the type of air-water interface was also dependent on the ventilation conditions upstream. The effect of slope also impacted the type of air-water interface, with zero slopes resulting in gravity current or gulping, and positive slope results in the near horizontal interface.

The numerical model was developed utilizing the rigid column theory and it applied to cases of ventilation greater than zero and discharge orifice size less than full discharge. With regards to pressure variations in pipelines, the numerical model worked well for discharge orifice $A_o^* = 0.0625$ and for discharge orifice $A_o^* = 0.25$ it did not work so well for conditions where ventilation was type 2 lower. For the cases where the model was not accurate, it over estimated the negative pressure. Another source of inaccuracy was the human error associated with the opening of the valves. The actual valve opening takes a few seconds where else the model predicts a sudden opening of the valve. This caused the results at the initial stages for of flow to be different for the model and the experimental work. The model predicted the outflows accurately. The were however minor discrepancies with the 0.1 slope caused by data collection errors due to the very fast flow rates experienced when collecting this data.

This research was limited because it considered a single straight pipe of constant diameter. Future research in this field can work with mixed diameter pipe or a network of pipes to evaluate how these affect the interface formations and pressure variations. The model used can also be improved to cater for a wider range of cases including no ventilation and full pipe discharge.

Bibliography

Alves, I. N., Shoham, O., and Taitel, Y. J. C. e. s. (1993). "Drift velocity of elongated bubbles in inclined pipes." 48(17), 3063-3070.

Baines, W. D. J. J. o. H. E. (1991). "Air cavities as gravity currents on slope." 117(12), 1600-1615.

Balacco, G., Apollonio, C., Piccinni, A. F. J. J. o. A. W. E., and Research (2015). "Experimental analysis of air valve behaviour during hydraulic transients." 3(1), 3-11.

Bashiri-Atrabi, H., Hosoda, T., and Shirai, H. J. J. o. H. E. (2016). "Propagation of an air-water interface from pressurized to free-surface flow in a circular pipe." 142(12), 04016055.

Bendiksen, K. H. J. I. j. o. m. f. (1984). "An experimental investigation of the motion of long bubbles in inclined tubes." 10(4), 467-483.

Benjamin, T. B. J. J. o. F. M. (1968). "Gravity currents and related phenomena." 31(2), 209-248.

Clanet, C., and Searby, G. J. J. o. F. M. (2004). "On the glug-glug of ideal bottles." 510, 145-168.

Coronado-Hernández, O. E., Fuertes-Miquel, V. S., Besharat, M., and Ramos, H. M. J. W. (2017). "Experimental and numerical analysis of a water emptying pipeline using different air valves." 9(2), 98.

Coronado-Hernández, O. E., Fuertes-Miquel, V. S., Iglesias-Rey, P. L., and Martínez-Solano, F. J. J. J. o. H. E. (2018). "Rigid water column model for simulating the emptying process in a pipeline using pressurized air." 144(4), 06018004.

Fuertes-Miquel, V. S., Coronado-Hernández, O. E., Iglesias-Rey, P. L., and Mora-Meliá, D. J. J. o. H. R. (2019). "Transient phenomena during the emptying process of a single pipe with water–air interaction." 57(3), 318-326.

Geiger, F., Velten, K., and Methner, F.-J. J. J. o. f. e. (2012). "3D CFD simulation of bottle emptying processes." 109(3), 609-618.

Gregory, G., and Scott, D. J. A. J. (1969). "Correlation of liquid slug velocity and frequency in horizontal cocurrent gas-liquid slug flow." 15(6), 933-935.

Izquierdo, J., Fuertes, V., Cabrera, E., Iglesias, P., and Garcia-Serra, J. J. J. o. h. r. (1999). "Pipeline start-up with entrapped air." 37(5), 579-590.

Kordestani, S., and Kubie, J. J. I. j. o. m. f. (1996). "Outflow of liquids from single-outlet vessels." 22(5), 1023-1029.

Laanearu, J., Annus, I., Koppel, T., Bergant, A., Vučković, S., Hou, Q., Tijsseling, A. S., Anderson, A., and van't Westende, J. M. J. J. o. H. E. (2012). "Emptying of large-scale pipeline by pressurized air." 138(12), 1090-1100.

Li, L., Zhu, D. Z. J. W. S., and Technology (2018). "Modulation of transient pressure by an air pocket in a horizontal pipe with an end orifice." 77(10), 2528-2536.

Liou, C. P., and Hunt, W. A. J. J. o. H. E. (1996). "Filling of pipelines with undulating elevation profiles." 122(10), 534-539.

McQuillan, K., and Whalley, P. J. I. J. o. M. F. (1985). "Flow patterns in vertical two-phase flow." 11(2), 161-175.

Mer, S., Praud, O., Neau, H., Merigoux, N., Magnaudet, J., and Roig, V. J. I. J. o. M. F. (2018). "The emptying of a bottle as a test case for assessing interfacial momentum exchange models for Euler–Euler simulations of multi-scale gas-liquid flows." 106, 109-124.

Nicholson, M., Aziz, K., and Gregory, G. J. T. C. J. o. c. e. (1978). "Intermittent two phase flow in horizontal pipes: predictive models." 56(6), 653-663.

Press, W. H., Press, W. H., Flannery, B. P., Teukolsky, S. A., Vetterling, W. T., Flannery, B. P., and Vetterling, W. T. (1989). *Numerical recipes in Pascal: the art of scientific computing*, Cambridge university press.

Trindade, B. C., and Vasconcelos, J. G. J. J. o. h. e. (2013). "Modeling of water pipeline filling events accounting for air phase interactions." 139(9), 921-934.

Weber, M. E., Alarie, A., and Ryan, M. E. J. C. e. s. (1986). "Velocities of extended bubbles in inclined tubes." 41(9), 2235-2240.

Weber, M. E., and ME, W. (1981). "Drift in intermittent two-phase flow in horizontal pipes."

Xue, C., and Zheng, Y. "Numerical calculation of air pressure changes in water filling and emptying process of pressured-pipeline with combined air valves." *Proc., 2011 International Conference on Electrical and Control Engineering*, IEEE, 1633-1636.

Zhou, F., Hicks, F., and Steffler, P. J. J. o. H. E. (2002). "Transient flow in a rapidly filling horizontal pipe containing trapped air." 128(6), 625-634.

Zukoski, E. J. J. o. F. M. (1966). "Influence of viscosity, surface tension, and inclination angle on motion of long bubbles in closed tubes." 25(4), 821-837.